UNIFORMLY HIGH-ORDER ACCURATE NON-OSCILLATORY SCHEMES I.

BY

AMI HARTEN [1]

SCHOOL OF MATHEMATICAL SCIENCES, TEL-AVIV UNIVERSITY

AND DEPT. OF MATHEMATICS, UCLA

STANLEY OSHER [2]

DEPT. OF MATHEMATICS, UCLA

(NASA-CR-181173) NUMERICAL SOLUTION OF THE UNSTEADY NAVIER-STOKES EQUATION Semiannual Report (California Univ.) 61 p Avail: NTIS HC A04/MF A01 CSCL 20D

N87-25546

Unclas

G3/34 0085370

1) Research supported by ARO Contract #DAAG -29-80 C-0041 while in Residence at the MRC, University of Wisconsin, and by NASA Consortium Agreement #NCA2-IR390-403 and ARO Grant # DAAG 29-82-0090 while at UCLA.

2) Research supported by NSF Grant #82-00788, ARO Grant #DAAG 29-82-0090, NASA-Consortium Agreement #NCA2-IR390-403, and NASA Langley Grants # NAG 1-270, and NAGI-506.

Abstract. We begin the construction and the analysis of nonoscillatory shock capturing methods for the approximation of hyperbolic conservation laws. These schemes share many desirable properties with total variation diminishing schemes, but TVD schemes have at most first order accuracy, in the sense of truncation error, at extrema of the solution. In this paper we construct a uniformly second order approximation, which is nonoscillatory in the sense that the number of extrema of the discrete solution is not increasing in time. This is achieved via a nonoscillatory piecewise linear reconstruction of the solution from its cell averages, time evolution through an approximate solution of the resulting initial value problem, and averaging of this approximate solution over each cell.

AMS-MOS Classification: Primary 65 M1O, Secondary 65 M05
Key Words: Conservation Laws, Finite Difference Scheme, Nonoscillatory, TVD.

1. Introduction. In this paper we consider numerical approximations to weak solutions of the scalar initial value problem (IVP)

(1.1a) $$u_t + f(u)_x = u_t + a(u)\, u_x = 0$$

(1.1b) $$u(x,0) = u_0(x) \ .$$

The initial data $u_0(x)$ are assumed to be piecewise-smooth functions that are either periodic or of compact support.

Let $v_j^n = v_h(x_j, t_n)$, $x_j = jh$, $t_n = n\tau$, denote a numerical approximation in conservation form

(1.2a) $$v_j^{n+1} = v_j^n - \lambda(\hat{f}_{j+1/2} - \hat{f}_{j-1/2}) \equiv (E_h \cdot v^n)_j$$

Here E_h is the numerical solution operator, $\lambda = \tau/h$, and $\hat{f}_{j+1/2}$, the numerical flux is a function of $2k$ variables

(1.2b) $$\hat{f}_{j+1/2} = \hat{f}(v_{j-k+1}^n, \ldots, v_{j+k}^n)$$

which is consistent with (1.1a) in the sense that

(1.2a) $$\hat{f}(u,u,\ldots,u) = f(u) \ .$$

We consider the numerical approximation $v_h(x,t)$ in (1.2) to be a piecewise-constant function

(1.3) $$v_h(x,t) = v_j^n, \quad x_{j-1/2} < x < x_{j+1/2}, \quad n\tau < t \le (n+1)\tau \ .$$

Accordingly we define its total variation in x to be

(1.4) $$TV(v^n) = TV(v_h(\cdot,t_n)) = \sum_j |v_{j+1}^n - v_j^n| \ .$$

If the total variation of the numerical solution is uniformly bounded in h for $0 \leq t \leq T$

$$(1.5) \qquad TV(v_h(\cdot,t)) \leq C \cdot TV(u_0)$$

then any refinement sequence $h \to 0$, $\tau = O(h)$ has a subsequence $h_j \to 0$ so that

$$(1.6) \qquad v_{h_j} \xrightarrow{L_1} u$$

where u is a weak solution of (1.1).

If all limit solutions (1.6) of the numerical solution (1.2) satisfy an entropy condition that implies uniqueness of the IVP (1.1), then the numerical scheme is convergent (see e.g [3], [12]).

Recently we have introduced the notion of total variation diminishing (TVD) schemes (see [3]), where the approximate solution operator is required to diminish the total variation (1.4) of the numerical solution at each time-step

$$(1.7) \qquad TV(v^{n+1}) \leq TV(v^n) ;$$

these schemes trivially satisfy (1.5) with $C = 1$. Some early work along these lines was done by van Leer in [15].

TVD schemes are non-oscillatory in the sense that the number of local extrema in the numerical solution is diminishing in time (as is customary we use "diminishing" loosely as short for "non-increasing", throughout this paper). Moreover, the value of an isolated local maximum may only decrease in time, while that of a local minimum may only increase.

We were able to construct TVD schemes that in the sense of local truncation error are high-order accurate everywhere except at local extrema where they necessarily degenerate into first-order accuracy (see [4], [13], [10], [11], [14]). The perpetual damping of local extrema determines the cumulative global error of the "high-order TVD schemes" to be $O(h)$ in the L_∞ norm, $O(h^{3/2})$ in the L_2 norm and $O(h^2)$ in the L_1 norm (see [17]).

In this paper we introduce a larger class of non-oscillatory schemes, in which the solution operator is only required to diminish the *number* of local extrema in the numerical solution. Unlike TVD schemes, which are a subset of this class, non-oscillatory schemes are not required to damp the values of each local extremum at every single time-step, but are allowed to occasionally accentuate a local extremum.

In a sequence of papers, of which the present paper is the first, we show how to construct non-oscillatory schemes that are uniformly high-order accurate (in the sense of global error for smooth solutions of (1.1)). In this first paper we describe a second-order accurate scheme of this type.

The fact that the number of local extrema in the numerical solution may only diminish in time is sufficient by itself to guarantee that the application of the scheme to monotone data results in a monotone function. Thus non-oscillatory schemes, like TVD schemes, are monotonicity preserving. In particular, when applied to a step-function, they do not generate spurious oscillations.

We note that since the number of local extrema in the solution of non-oscillatory schemes is bounded by that of the initial data, uniform boundedness of its total variation (1.5) follows immediately if the maximum norm of the solution is shown to be uniformly bounded.

2. Design Principle and Overview

In this section we describe how to construct a non-oscillatory scheme that is uniformly second-order accurate.

Integrating the partial differential equation (1.1a) over the computational cell $(x_{j-1/2}, x_{j+1/2}) \times (t_n, t_{n+1})$ we get

(2.1a) $$\bar{u}_j^{n+1} = \bar{u}_j^n - \lambda[\hat{f}_{j+1/2}(u) - \hat{f}_{j-1/2}(u)]$$

where

(2.1b) $$\hat{f}_{j+1/2}(u) = \frac{1}{\tau} \int_{t_n}^{t_{n+1}} f(u(x_{j+1/2}, t))\, dt \, ,$$

and

(2.1c) $$\bar{u}_j^n = \frac{1}{h} \int_{x_{j-1/2}}^{x_{j+1/2}} u(x,t_n)\, dx \, .$$

We observe that although (2.1a) is a relation between the cell-averages $\bar{u}_j^n$ and $\bar{u}_j^{n+1}$, the evaluation of the fluxes $\hat{f}_{j+1/2}(u)$ in (2.1b) requires knowledge of the solution itself and not its cell-averages.

As in Godunov's scheme and its second-order extension by van Leer [16] and Colella and Woodward [2], we derive our scheme as a direct approximation to (2.1). We denote by v_j^n the numerical approximation to the cell-averages $\bar{u}_j^n$ of the exact solution in (2.1c), and set v_j^0 to be the cell-averages of the initial data. Given $v^n = \{v_j^n\}$ we compute v^{n+1} as follows:

First we reconstruct $u(x,t_n)$ out of its approximate cell-averages $\{v_j^n\}$ to the appropriate accuracy and denote the result by $L(x; v^n)$. Next we solve the IVP

(2.2) $$v_t + f(v)_x = 0, \;\; v(x,0) = L(x; v^n)$$

and denote its solution by $v(x,t)$. Finally we obtain v_j^{n+1} by taking cell-averages of $v(x,\tau)$

(2.3) $$v_j^{n+1} = \frac{1}{h} \int_{x_{j-1/2}}^{x_{j+1/2}} v(x,\tau)\, dx .$$

The averaging operator in (2.3) is non-oscillatory, therefore the number of local extrema in v^{n+1} (interpreted as a mesh-function or the piecewise-constant function (1.3)) does not exceed that of $v(x,\tau)$. Assuming $v(x,t)$ to be the exact solution of (2.2) implies (since the exact solution operator is TVD) that the number of local extrema in $v(x,\tau)$ is less than or equal to that of $v(x,0) = L(x; v^n)$. Therefore if the number of local extrema in $L(x; v^n)$ does not exceed that of v^n, then the resulting scheme is non-oscillatory.

We conclude that the design of non-oscillatory high order accurate schemes essentially boils down to a problem on the level of approximation of functions: Given cell-averages $\bar{u}_j$ of a piecewise-smooth function $u(x)$, reconstruct $u(x)$ to a desired accuracy. Prior to studying this problem we tackle another related question in approximation of functions, that of constructing a non-oscillatory high-order accurate interpolation of piecewise-smooth functions.

In section 3 we construct a non-oscillatory piecewise-parabolic function $Q(x; u)$ that interpolates a piecewise-smooth function $u(x)$ at the mesh points

(2.4a) $$Q(x_j; u) = u(x_j)$$

and satisfies, wherever $u(x)$ is smooth,

(2.4b) $$Q(x; u) = u(x) + O(h^3)$$

(2.4c) $$\frac{d}{dx} Q(x \pm 0; u) = \frac{d}{dx} u(x) + O(h^2) .$$

In section 4 we make use of this non-oscillatory piecewise-parabolic interpolant to design a non-oscillatory reconstruction of a piecewise-smooth function from its cell-averages. As in [16], [2], [5], and [9] we take $L(x;\bar{u})$ to be the following piecewise-linear function

(2.5a) $$L(x;\bar{u}) = \bar{u}_j + S_j(x - x_j)/h \quad \text{for} \quad |x - x_j| < h/2 .$$

Unlike the above references that present "second-order accurate" TVD schemes, we compute the slopes S_j/h from $Q(x;\bar{u})$ by

(2.5b) $$S_j/h = m\left(\frac{d}{dx} Q(x_j - 0;\bar{u}),\ \frac{d}{dx} Q(x_j + 0;\bar{u})\right) .$$

Here $m(x,y)$ is the min mod function

(2.6) $$m(x,y) = \begin{cases} s \cdot \min(|x|,|y|) & \text{if } \operatorname{sgn}(x) = \operatorname{sgn}(y) = s \\ 0 & \text{otherwise} \end{cases}$$

We show in section 4 that $L(x;\bar{u})$ is a proper reconstruction of $u(x)$ in the sense that whenever $u(x)$ is smooth

(2.7a) $$L(x;\bar{u}) = u(x) + O(h^2)$$

and

(2.7b) $$\bar{L}(x;\bar{u}) = \bar{u}(x) + O(h^3) .$$

Here $\bar{u}(x) = h^{-1} \int_{-h/2}^{h/2} u(x + y)\, dy$ and $\bar{L}(x;\bar{u}) = h^{-1} \int_{-h/2}^{h/2} L(x + y;\bar{u})\, dy$; like $Q(x;\bar{u})$, the latter is also a non-oscillatory piecewise-parabolic interpolant of $\bar{u}(x)$,

(2.7c) $$\bar{L}(x_j;\bar{u}) = \bar{u}(x_j) .$$

We remark that the "second-order accurate" TVD schemes described in the above mentioned references use a slope S_j/h in (2.5a) that approximates $(d/dx)\, u(x_j)$ to $O(h)$, and their loss of second-order accuracy at local extrema points is due to lack of smoothness of the coefficient in the $O(h)$ term at these points [1]. This problem is circumvented in the present scheme by taking S_j/h to be (2.5b) which is an $O(h^2)$ approximation to $(d/dx)\, u(x_j)$. Unfortunately there is a price to pay for this extra accuracy, namely the loss of the TVD property. As in TVD schemes

$$TV(v^{n+1}) \leq TV(L(\cdot\,; v^n)) \,, \tag{2.8}$$

however here

$$TV(L(\cdot\,; v^n)) \geq TV(v^n)$$

and indeed the scheme may occasionally increase the variation of the numerical solution. Although we prove that the scheme is non-oscillatory we have not been able as yet to complete a proof of uniform boundedness of the total variation of the numerical solution; this is due to lack of techniques to verify uniform boundedness of the maximum norm of the numerical solution.

In section 5 we study the proposed scheme in the constant coefficient case. We verify that it is uniformly second-order accurate, examine its behavior at local extrema points and get estimates for the possible increase in total variation per time-step.

In this paper where we consider numerical schemes of the form (1.2) that are

1. We repeat that the results of [8] and [11] imply that TVD schemes, no matter how they are constructed, must have this loss of accuracy at local extrema

derived from approximating the relation (2.1), it is only natural to consider truncation error in the sense of cell-averages, i.e. we say that the scheme (1.2) is second-order accurate if

$$\bar{u}^{n+1} = E_h \cdot \bar{u}^n + O(h^3) \tag{2.9}$$

where $\bar{u}^n$ is the cell-average (2.1c) of the exact solution. Since

$$\bar{u}(x) = u(x) + O(h^2) \tag{2.10}$$

whenever $u(x)$ is smooth, (2.9) holds also for pointwise values of the solution. However, in the context of 3rd and higher order accurate schemes, this difference in definitions of truncation error will be not only conceptual but of practical importance as well.

Up to this point we have assumed that $v(x,\tau)$ in (2.3) is the exact solution to (2.2). The resulting scheme

$$v_j^{n+1} = v_j^n - \lambda[\hat{f}_{j+1/2}(v) - \hat{f}_{j-1/2}(v)] , \tag{2.11a}$$

where $\hat{f}_{j+1/2}(v)$ is (2.1b) applied to $v(x,t)$,

$$\hat{f}_{j+1/2}(v) = \frac{1}{\tau} \int_0^\tau f(v(x,t))\, dt , \tag{2.11b}$$

is certainly second-order accurate in the sense of (2.9). Starting with the exact cell-averages $v_j^n = \bar{u}_j^n$ in (2.11) we get from (2.7a) that

$$v(x,t) = u(x,t + t_n) + O(h^2) \quad \text{for} \quad 0 \le t \le \tau \tag{2.12a}$$

and consequently

$$\hat{f}_{j+1/2}(v) = \hat{f}_{j+1/2}(u) + O(h^2) , \tag{2.12b}$$

which implies (2.9) due to the sufficient smoothness of the coefficient in the

$O(h^2)$ term in (2.12b).

In section 6 we replace the exact solution $v(x,t)$ in (2.3) by an approximate one, which we denote by $v_n(x,t)$. This approximate solution is conservative, TVD, and second-order accurate in the sense of (2.12a). Thus replacing $v(x,t)$ in (2.3) by this approximate solution results in a conservative scheme that is non-oscillatory and uniformly second order accurate.

We remark that an alternative approach to the above is to approximate $\hat{f}_{j+1/2}(v)$ in (2.11b) by using a midpoint rule (or trapezoidal rule) for the integral and by replacing $v(x,t)$ with a non-oscillating second-order accurate approximate one $v_n(x,t)$ (see [16] and [2]). The resulting scheme

(2.13a) $$v_j^{n+1} = v_j^n - \lambda(\hat{f}_{j+1/2} - \hat{f}_{j-1/2})$$

(2.13b) $$\hat{f}_{j+1/2} = f(v_n(x_{j+1/2}, \tau/2))$$

is certainly second-order accurate, and it is non-oscillatory in the constant coefficient case. Since we have not used the cell-averaging (2.3) to derive this scheme, we cannot ascertain in general that the resulting scheme is non-oscillatory. Nevertheless, our numerical experiments as well as many other experiments in the context of TVD schemes (see e.g. [1], [2]) demonstrate that the numerical results are non-oscillatory in many (if not all) applications.

In section 7 we present some numerical experiments that compare the present scheme with a typical "second-order accurate" TVD scheme.

3. Nonoscillatory interpolation.

The oscillatory nature of second order accurate Lax-Wendroff type schemes results from a Gibbs phenomenon associated with high-order interpolation across discontinuities. In this section, as a preparatory step towards designing a nonoscillatory approximation to (1.1.), we construct a non-oscillatory piecewise-parabolic interpolant $Q(x; u)$ to a piecewise-smooth function $u(x)$ such that

(3.1a) $$Q(x_i; u) = u(x_i)$$

(3.1b) $$Q(x; u) = q_{i+1/2}(x; u), \quad x_i \le x \le x_{i+1},$$

where $q_{i+1/2}$ is a quadratic polynomial, and

(3.1c) $$Q(x; u) - u(x) = O(h^3), \ \frac{d}{dx} Q(x \pm 0; u) - \frac{d}{dx} u(x) = O(h^2)$$

wherever $u(x)$ is smooth.

$Q(x; u)$ is non-oscillatory in the sense that the number of its local extrema does not exceed that of $u(x)$.

Since

$$q_{i+1/2}(x_i; u) = u_i, \quad q_{i+1/2}(x_{i+1}; u) = u_{i+1}$$

it can be written in the form

(3.2a) $$q_{i+1/2}(x;u) = u_i + d_{i+1/2}\, u \cdot (x - x_i)/h + \frac{1}{2} D_{i+1/2}\, u \cdot (x - x_i)(x - x_{i+1})/h^2$$

where

(3.2b) $$d_{i+1/2}\, u = u_{i+1} - u_i$$

and $D_{i+1/2}\, u$ is yet to be determined.

$$D_{i+1/2}\, u = h^2\, q''_{i+1/2}(x; u), \quad x_i \le x \le x_{i+1}.$$

We consider as candidates for $q_{i+1/2}$ the two quadratic polynomials $\bar{q}_i$ and $\bar{q}_{i+1}$, interpolating $u(x)$ at (x_{i-1}, x_i, x_{i+1}) and (x_i, x_{i+1}, x_{i+2}), respectively, and choose $q_{i+1/2}$ to be the one that is least oscillatory in $[x_i, x_{i+1}]$. Both $\bar{q}_j$, $j = i$ and $j = i+1$, can be written as (3.2a) with $D_{i+1/2}\, u = D_j u$ where

(3.2c) $$D_j u = d_{j+1/2} u - d_{j-1/2} u = u_{j+1} - 2u_j + u_{j-1} .$$

Since the least oscillatory of $\bar{q}_i$ and $\bar{q}_{i+1}$ can be characterized as the one that deviates the least from the line connecting (x_i, u_i) with (x_{i+1}, u_{i+1}) we choose $D_{i+1/2}\, u$ in (3.2a) to be

(3.2d) $$D_{i+1/2}\, u = m(D_i u, D_{i+1} u) ,$$

where $m(x,y)$ is the min mod function

(3.3) $$m(x,y) = \begin{cases} s \cdot \min(|x|,|y|), & \text{if } \operatorname{sgn}(x) = \operatorname{sgn}(y) = s \\ 0 & \text{otherwise.} \end{cases}$$

If $u(x)$ is smooth in $[x_{j-1}, x_{j+1}]$, then $\bar{q}_j$ as a quadratic interpolant of u satisfies

(3.4) $$\bar{q}_j(x) - u(x) = O(h^3), \quad \frac{d}{dx}\bar{q}_j(x) - \frac{d}{dx}u(x) = O(h^2), \quad x_{j-1} \le x \le x_{j+1} .$$

If $D_i u \cdot D_{i+1} u \ge 0$ then $q_{i+1/2}$ is either $\bar{q}_i$ or $\bar{q}_{i+1}$. Otherwise we set $D_{i+1/2}\, u = 0$, but then smoothness of u implies that $D_j u = O(h^3)$ and consequently $q_{i+1/2} - \bar{q}_j = O(h^3)$ for $j = i, i+1$. Thus (3.1c) follows from (3.4).

We turn now to prove that $Q(x; u)$ is a nonoscillatory interpolant of u, i.e. that the number of its local extrema does not exceed that of u. We do so by showing a one-to-one correspondence between local extrema of Q to those of the mesh function $\{u_j\}$, the number of which certainly does not exceed that of $u(x)$.

Q may have a local extremum in either the interior of some interval (x_i, x_{i+1}) or at a mesh point x_i. The first case, which will be refered to as interior-extremum, occurs when there is a point x^*, $x_i < x^* < x_{i+1}$, such that

$$\frac{d}{dx} Q(x^*; u) = 0, \text{ but } \frac{d}{dx} q_{i+1/2} \neq 0 .$$

From (3.2a) if follows that Q has an interior-extremum, in (x_i, x_{i+1}) if and only if

(3.5) $$|D_{i+1/2}\, u| > 2|d_{i+1/2}\, u| .$$

$q^*_{i+1/2} = q_{i+1/2}(x^*)$, the value of the interior-extremum is then

(3.6) $$q^*_{i+1/2} = u_i - \frac{1}{2} D_{i+1/2} u \cdot \left(\frac{d_{i+1/2}\, u}{D_{i+1/2}\, u} - \frac{1}{2} \right)^2 ;$$

if $D_{i+1/2}\, u < 0$ it is a local maximum; if $D_{i+1/2}\, u > 0$ it is a local minimum. Since $D_{i+1/2} u = m(D_i u, D_{i+1}\, u)$, (3.5) holds if and only if

(3.7a) $$D_i\, u \cdot D_{i+1} u > 0$$

(3.7b) $$|D_j\, u| > 2|d_{i+1/2}\, u|, \quad j = i,\, i+1 .$$

This implies that $q_{i+1/2}$ has a local extremum in (x_i, x_{i+1}) if and only if *both* $\bar{q}_i$ and $\bar{q}_{i+1}$ also have a local extremum in (x_i, x_{i+1}) and of the same kind. Since a parabola has at most one local extremum, it follows then that $\bar{q}_i$ does not have a local extremum in (x_{i-1}, x_i) and $\bar{q}_{i+1}$ does not have one in (x_{i+1}, x_{i+2}). Consequently Q is monotone in both (x_{i-1}, x_i) and (x_{i+1}, x_{1+2}), but in an opposite sense, i.e. $d_{i-1/2}\, u \cdot d_{i+3/2}\, u < 0$; the latter implies that u has a local extremum in $[x_i, x_{i+1}]$ and that either u_i or u_{i+1} is a local extremum of the mesh function $\{u_j\}$ (for obvious reasons the case $u_i = u_{i+1}$ is counted as a single-extremum). The above analysis also shows that interior-extrema are isolated, i.e. if Q has an interior-extremum in (x_i, x_{i+1}), then it is the only local extremum of Q in (x_{i-1}, x_{i+2}).

We turn now to examine the case that Q has a local extremum at a mesh point x_i; this will be refered to as a mesh-extremum. The above observation that interior extrema are isolated excludes the possibility that Q has an interior-extremum in either (x_{i-1}, x_i) or (x_i, x_{i+1}) and consequently Q is monotone in these intervals. This implies that $d_{i-1/2}\, u \cdot d_{i+1/2}\, u < 0$ and therefore u_i is a local extremum of the mesh function $\{u_j\}$. This concludes the proof that $Q(x; u)$ is a non-oscillatory interpolant of u.

We next express the non-oscillatory nature of Q in terms of total variation. If $|D_{j+1/2}\, u| \le 2|d_{j+1/2}\, u|$ then (2.5) implies that Q is monotone in $[x_j, x_{j+1}]$. Thus

(3.8a) $$|D_{j+1/2}\, u| \le 2|d_{j+1/2}\, u| \Rightarrow TV_{[x_j,x_{j+1}]}(Q) = |d_{j+1/2}\, u| .$$

If $|D_{j+1/2}\, u| > 2|d_{j+1/2}\, u|$ then Q has a local extremum in (x_j, x_{j+1}) and

$$TV_{[x_j,x_{j+1}]}(Q) = |q^*_{j+1/2} - u_j| + |u_{j+1} - q^*_{j+1/2}| .$$

Using (2.6) we get

(3.8b) $$|D_{j+1/2}\, u| > 2|d_{j+1/2}\, u| \Rightarrow TV_{[x_j,x_{j+1}]}(Q)$$

$$= |d_{j+1/2}\, u| + |D_{j+1/2}\, u| \left(\left| \frac{d_{j+1/2}\, u}{D_{j+1/2}\, u} \right| - \frac{1}{2} \right)^2 .$$

We conclude that

$$(3.8c)\quad 0 \le TV(Q) - \sum_j |d_{j+1/2}\, u| \le \sum_{m \in M} |D_{m+1/2}\, u| \left(\left| \frac{d_{m+1/2}\, u}{D_{m+1/2}\, u} \right| - \frac{1}{2} \right)^2$$

$$\le \frac{1}{4} \sum_{m \in M} |D_{m+1/2}\, u| \, .$$

The sum in the RHS of (3.8c) is taken over the set of indices M of intervals (x_m, x_{m+1}) in which $|D_{m+1/2}\, u| > 2|d_{m+1/2}\, u|$, i.e. where Q has interior-extrema.

Next we show that if $u(x)$ is a piecewise-smooth function of bounded variation, then

$$(3.9)\qquad \lim_{h \to 0} TV(Q(\cdot\,; u)) = TV(u) \, .$$

We observe that in this case the number of intervals in M is finite and is uniformly bounded by the number of local extrema in $u(x)$. Hence (3.9) will follow if we prove that $D_{m+1/2}\, u \to 0$ as $h \to 0$ for all $m \in M$. To accomplish this we show that for h sufficiently small M does not include intervals (x_m, x_{m+1}) in which $u(x)$ is discontinuous. To see that let us examine the case where $u(x)$ has a discontinuity at $\bar{x} \in (x_i, x_{i+1})$. Clearly $d_{i+1/2}\, u$ approaches the size of the jump in u while $d_{i-1/2} u$ approaches zero as $h \to 0$. Consequently

$$(3.10a)\qquad |D_i u / d_{i+1/2}\, u| = |1 - d_{i-1/2} u / d_{i+1/2}\, u| \to 1 \quad \text{as} \quad h \to 0$$

Hence for h sufficiently small

$$(3.10b)\qquad 2|d_{i+1/2}\, u| > |D_i\, u| \ge |D_{i+1/2}\, u|$$

which implies $i \notin M$.

4. Non-oscillatory Reconstruction.

Let $u(x)$ be a piecewise-smooth function and denote by $\bar{u}(x)$ its mean over $(x - h/2, x + h/2)$, i.e.

(4.1) $$\bar{u}(x) = \frac{1}{h} \int_{x-h/2}^{x+h/2} u(y)\, dy .$$

We denote $\bar{u}_j = \bar{u}(x_j)$ and refer to these values as cell-averages of $u(x)$. Given $\{\bar{u}_j\}$, the task in hand is to reconstruct $u(x)$ to $O(h^2)$ in a non-oscillatory way; denote the approximately reconstructed function by $L(x; \bar{u})$. To achieve $O(h^2)$ accuracy it is sufficient to consider $L(x; \bar{u})$ to be a piecewise-linear function. To make $L(x; \bar{u})$ a non-oscillatory approximation we use the non-oscillatory piecewise parabolic interpolation $Q(x; \bar{u})$ to compute its slopes as follows:

(4.2a) $$L(x; \bar{u}) = \bar{u}_j + S_j(x - x_j)/h \quad \text{for} \quad |x - x_j| < \frac{1}{2} h$$

(4.2b) $$S_j = h \cdot m\left(\frac{d}{dx} Q(x_j - 0; \bar{u}),\ \frac{d}{dx} Q(x_j + 0; \bar{u}) \right) .$$

Here m is the min mod function (3.3); $d_{i+1/2}\, \bar{u}$ and $D_{i+1/2}\, \bar{u}$ are (3.2b) and (3.2d), respectively.

We note that $L(x; \bar{u})$ may be discontinuous at $\{x_{j+1/2}\}$ and that

(4.3a) $$L(x_j; \bar{u}) = \bar{u}_j .$$

To see that wherever $u(x)$ is smooth

(4.3b) $$L(x,\bar{u}) - u(x) = O(h^2)$$

we observe that in this case

(4.4a) $$\bar{u}(x) = u(x) + O(h^2)$$

and therefore it follows from (3.1c) that

(4.4b) $$\frac{1}{h} S_j = \frac{d}{dx} \bar{u}(x_j) + O(h^2) = \frac{d}{dx} u(x_j) + O(h^2) .$$

Consequently the RHS of (4.2a) can be expanded as

(4.4c) $$L(x; \bar{u}) = u_j + (x - x_j) \frac{d}{dx} u(x_j) + O(h^2)$$

$$= u(x) + 0(h^2) \quad \text{for } |x - x_j| < \frac{1}{2} h$$

and thus (4.3b) follows.

Denote by $\bar{L}(x; \bar{u})$ the mean value of $L(x; \bar{u})$ in $(x - h/2, x + h/2)$, i.e.

(4.5a) $$\bar{L}(x; \bar{u}) = \frac{1}{h} \int_{x-h/2}^{x+h/2} L(y; \bar{u})\, dy .$$

Using (4.2a) to evaluate the integral in (4.5a) we find

(4.5b) $$\bar{L}(x; \bar{u}) = \bar{u}_j + d_{j+1/2}\, \bar{u}$$

$$\cdot (x - x_j)/h + (1/2)(S_{j+1} - S_j)(x - x_j)(x - x_{j+1})/h^2,$$

for $x_j \leq x \leq x_{j+1}$

(4.5c) $$\bar{L}(x_j; \bar{u}) = \bar{u}_j .$$

Hence $\bar{L}(x; \bar{u})$, like $Q(x; \bar{u})$, is a piecewise-parabolic interpolant of $\bar{u}(x)$. Comparing (4.5b) with (3.2) we find that for $x_j \leq x \leq x_{j+1}$

(4.6a) $$\bar{L}(x; \bar{u}) - Q(x; \bar{u}) = \frac{1}{2}(S_{j+1} - S_j - D_{j+1/2}\, \bar{u})(x - x_j)(x - x_{j+1})/h^2 .$$

From (4.4b) we see that $S_i = h \frac{d}{dx} \bar{u}(x_i) + O(h^3)$ (Note that this is true also at local extrema points) and therefore

$$S_{j+1} - S_j = h^2 \frac{d^2}{dx^2} u(x_{j+1/2}) + O(h^3) .$$

On the other hand (3.2) shows that

$$D_{j+1/2} \bar{u} = h^2 \frac{d^2}{dx^2} u(x_{j+1/2}) + O(h^3) .$$

Therefore

(4.6b) $$S_{j+1} - S_j - D_{j+1/2} \bar{u} = O(h^3)$$

which shows that RHS of (4.6a) is $O(h^3)$. Since (2.1c) shows that

$$Q(x; \bar{u}) - \bar{u}(x) = O(h^3)$$

we conclude from (4.6a)-(4.6b) that

(4.6c) $$\bar{L}(x; \bar{u}) - \bar{u}(x) = O(h^3) .$$

We turn now to prove that $L(x; \bar{u})$ is a non-oscillatory approximation to $\bar{u}(x)$; this certainly implies that $L(x; \bar{u})$ is a non-oscillatory approximation to $u(x)$. We shall do so by showing that $TV_{[x_j,x_{j+1}]}(L(\cdot; \bar{u}))$, the total-variation of $L(x; \bar{u})$ in $[x_j, x_{j+1}]$, which has the value

(4.7a) $$TV_{[x_j,x_{j+1}]}(L(\cdot; \bar{u})) = \frac{1}{2}(|S_j| + |S_{j+1}|) + |d_{j+1/2} \bar{u} - \frac{1}{2}(S_j + S_{j+1})| ,$$

can also be expressed as

(4.7b) $$TV_{[x_j,x_{j+1}]}(L(\cdot; \bar{u})) = \max(|d_{j+1/2} \bar{u}|, \frac{1}{2}|D_{j+1/2} \bar{u}|) .$$

Then it follows immediately form (4.7b), (4.3a) and (3.8) that L is monotone in $[x_j, x_{j+1}]$ if and only if Q is; consequently L is a non-oscillatory approximation to $u(x)$ in exactly the same sense as Q is to the interpolated function (see section 3).

Next let us denote

(4.8a) $$S_j^{\pm} = h \cdot \frac{d}{dx} Q(x_j \pm 0; \bar{u}) ,$$

i.e.

(4.8b) $$S_j^- = d_{j-1/2}\, \bar{u} + \frac{1}{2} D_{j-1/2}\, \bar{u}, \quad S_j^+ = d_{j+1/2}\, \bar{u} - \frac{1}{2} D_{j+1/2}\, \bar{u} ,$$

and observe that (4.2b) implies that

(4.8c) $$\frac{1}{2}(|S_j| + |S_{j+1}|) = \frac{1}{2}\left[|m(S_j^-, S_j^+)| + |m(S_{j+1}^-, S_{j+1}^+)|\right]$$

$$\leq \frac{1}{2}(|S_j^+| + |S_{j+1}^-|) = \frac{1}{2}\left(\left|d_{j+1/2}\, \bar{u} - \frac{1}{2} D_{j+1/2}\, \bar{u}\right| + \left|d_{j+1/2}\, \bar{u} + \frac{1}{2} D_{j+1/2}\, \bar{u}\right|\right)$$

$$= \max\left(|d_{j+1/2}\, \bar{u}|, \frac{1}{2}|D_{j+1/2}\, \bar{u}|\right) .$$

We note that if $|d_{j+1/2}\, \bar{u}| \geq 1/2|D_{j+1/2}\, \bar{u}|$ then

$$\operatorname{sgn}\left(d_{j+1/2}\, \bar{u} \pm \frac{1}{2} D_{j+1/2}\, \bar{u}\right) \cdot \operatorname{sgn}(d_{j+1/2}\, \bar{u}) \geq 0$$

which in turn implies

$$\operatorname{sgn}(S_j) \cdot \operatorname{sgn}(d_{j+1/2}\, \bar{u}) \geq 0, \quad \operatorname{sgn}(S_{j+1}) \cdot \operatorname{sgn}(d_{j+1/2}\, \bar{u}) \geq 0$$

It follows then from (4.8c) that the RHS of (4.7a) is $|d_{j+1/2}\, \bar{u}|$. This shows that

(4.9a) $$|d_{j+1/2}\, \bar{u}| \geq \frac{1}{2}\, |D_{j+1/2}\, \bar{u}| \Rightarrow TV_{[x_j, x_{j+1}]}(L(\cdot\, ; \bar{u})) = |d_{j+1/2}\, \bar{u}| .$$

To complete the verification of (4.7b) we still have to show that

$$(4.9b) \qquad |d_{j+1/2}\,\bar{u}| < \frac{1}{2}\,|D_{j+1/2}\,\bar{u}| \Rightarrow TV_{[x_j,x_{j+1}]}(L(\cdot\,;\bar{u})) = \frac{1}{2}\,|D_{j+1}\,\bar{u}|\,.$$

First we observe that

$$(4.10) \quad S_i^+ - S_i^- = (d_{i+1/2}\,\bar{u} - \frac{1}{2}\,D_{i+1/2}\,\bar{u}) - (d_{i-1/2}\,\bar{u} + \frac{1}{2}\,D_{i-1/2}\,\bar{u})\,.$$

$$= D_i\,\bar{u} - \frac{1}{2}(D_{i+1/2}\,\bar{u} + D_{i-1/2}\,\bar{u})$$

Since (3.2d) implies

$$(4.11) \qquad |D_i\,\bar{u}| \le \frac{1}{2}\,(|D_{i-1/2}\,\bar{u}| + |D_{i+1/2}\,\bar{u}|)$$

we conclude from (4.10) that

$$(4.12) \qquad (S_i^+ - S_i^-)\cdot \mathrm{sgn}(D_i\,\bar{u}) \ge 0\,.$$

We turn now to prove (4.9b). First let us consider the case that $Q(x;\bar{u})$ has a local maximum in (x_j, x_{j+1}), i.e. $D_j\,\bar{u} < 0$, $D_{j+1}\,\bar{u} < 0$, and $|d_{j+1/2}\,\bar{u}| < \frac{1}{2}\,|D_{j+1/2}\,\bar{u}|$.

It follows from (4.12) that

$$(4.13a) \qquad S_j^- \ge S_j^+ = d_{j+1/2}\,\bar{u} - \frac{1}{2}\,D_{j+1/2}\,\bar{u} > 0$$

$$(4.13b) \qquad 0 > d_{j+1/2}\,\bar{u} + \frac{1}{2}\,D_{j+1/2}\,\bar{u} = S_{j+1}^- \ge S_{j+1}^+\,.$$

The relations (4.13) and the definitions (4.8a), (4.2b) imply that

$$(4.14a) \qquad S_j = S_j^+ = d_{j+1/2}\,\bar{u} - \frac{1}{2}\,D_{j+1/2}\,\bar{u}$$

(4.14b) $$S_{j+1} = S_{j+1}^{-} = d_{j+1/2}\,\bar{u} + \frac{1}{2} D_{j+1/2}\,\bar{u}\,.$$

The same analysis shows that (4.14) holds also for the case that $Q(x;\bar{u})$ has a local minimum in (x_j, x_{j+1}). (4.9b) follows immediately from (4.14) and (4.7a).

We note that since $L(x;\bar{u})$ is continuous at x_j

(4.15) $$TV(L(\cdot;\bar{u})) = \sum_j TV_{[x_j,x_{j+1}]}(L(\cdot;\bar{u})) = \sum_j \max\left(|d_{j+1/2}\,\bar{u}|,\ \frac{1}{2}\,|D_{j+1/2}\,\bar{u}|\right)$$

$$= \sum_j |d_{j+1/2}\,\bar{u}| + \sum_{m\in M} \left(\frac{1}{2}\,|D_{m+1/2}\,\bar{u}| - |d_{m+1/2}\,\bar{u}|\right).$$

Here M is the set of indices of intervals (x_m, x_{m+1}) in the interior of which L (and also Q) has a local extremum. The number of these intervals is finite and is bounded by the number of local extrema of $\bar{u}(x)$. Comparing (4.9) with (3.8) we note that

(4.16) $$TV(L(\cdot;\bar{u})) \geq TV(Q(\cdot;\bar{u}))\,.$$

5. The constant coefficient case.

In this section we study the constant coefficient case

(5.1) $$u_t + au_x = 0, \quad a = \text{const}\,.$$

The exact solution of the IVP (2.2) is

(5.2) $$v(x,t) = L(x - at; v^n)\,.$$

Hence our scheme (2.3) is

(5.3a) $$v_j^{n+1} = \frac{1}{h}\int_{x_{j-1/2}}^{x_{j+1/2}} L(x - a\tau; v^n)\,dx = \bar{L}(x_j - a\tau; v^n)$$

where $\bar{L}$ is (4.5a). We have shown in section 3 that the number of local extrema in $L(x; v^n)$ does not exceed that of v^n. Since v^{n+1} in (5.3a) is a cell-average of L, it follows that the number of local extrema in v^{n+1} does not exceed that of v^n, and consequently the scheme (5.3a) is non-oscillatory.

Using (4.5b) in (5.3a) we get the following expression for the scheme

(5.3b) $v_j^{n+1} = (E_h \cdot v^n)_j$

$$= \begin{cases} v_j^n - \mu d_{j-1/2} v^n - 1/2\, \mu(1-\mu)(S_j^n - S_{j-1}^n) & \text{if } a > 0 \\ v_j^n - \mu d_{j+1/2} v^n + 1/2\, \mu(1+\mu)(S_{j+1}^n - S_j^n) & \text{if } a < 0 \end{cases};$$

E_h denotes the operator form of the finite difference scheme; $\mu = \lambda a$, the CFL-number, is assumed to satisfy

(5.3c) $$|\mu| \leq 1 .$$

We turn now to prove that (5.3) is second order accurate in the sense of (2.9), i.e. if $\bar{u}^n(x)$ denotes the mean value (4.1) of $u(x,t_n)$ then

(5.4a) $$\bar{u}_j^{n+1} - (E_h \cdot \bar{u}^n)_j = O(h^3) .$$

To show that we observe that in the constant coefficient case (5.1) $\bar{u}_j^{n+1} = \bar{u}^n(x_j - a\tau)$, and by (5.3a) $(E_h \cdot \bar{u}^n)_j = \bar{L}(x_j - a\tau; \bar{u}^n)$. Hence the LHS of (5.4a) is nothing but

(5.4b) $$\bar{u}^n(x_j - a\tau) - \bar{L}(x_j - a\tau; \bar{u}^n) ,$$

which is $O(h^3)$ as a direct consequence of (4.bc).

Next we study the time-dependence of the total variation and the maximum norm of the numerical solution (5.3). In section 2 we have pointed out that

(5.5a) $$TV(v^{n+1}) \le TV(L(\cdot\,; v^n)) \,.$$

Using (4.15) and (5.5a) we get the following upper bound on the possible growth of the total variation of the numerical solution per time-step

(5.5b) $$TV(v^{n+1}) - TV(v^n) \le \sum_{m \in M_n} \left(\frac{1}{2} |D_{m+1/2}\, v^n| - |d_{m+1/2}\, v^n| \right) .$$

Here M_n is the set of indices of intervals (x_m, x_{m+1}) in the interior of which $L(x; v^n)$ (and also $Q(x; v^n)$) has a local extremum. The number of these intervals is finite and remains uniformly bounded in time by the number of local extrema in the initial data.

Clearly the upper bound (5.5b) is overly pessimistic. It estimates the possible increase in variation in the reconstruction step due to replacing the cell-averages v_j^n by the piecewise-linear function $L(x; v^n)$. It does not take into account the possible decrease in variation in the averaging step (2.3), resulting from doing just the opposite, i.e. replacing the piecewise-linear function $L(x - a\tau; v^n)$ in (5.2) by its cell-averages (5.3a).

In the following we shall examine the temporal behaviour of the local extrema of the numerical solution and its total variation by analysing the explicit values of the cell-averages v_j^{n+1} given by (5.3b). To simplify our presentation let us assume that $a > 0$.

First we note that (4.8b) implies

(5.6a) $$|S_j - S_{j-1}| \le |S_j| + |S_{j+1}| \le 2 \max(|d_{j-1/2}\, v^n|, \frac{1}{2} |D_{j-1/2} v^n|) \,.$$

Hence

(5.6b) $|d_{j-1/2}\, v^n| \geq \frac{1}{2}\, |D_{j-1/2}\, v^n| \Rightarrow |\gamma_{j-1/2}| = |S_j^n - S_{j-1}^n| / |d_{j-1/2}\, v^n| \leq 2$.

Rewriting (5.3) in this case as

(5.7a) $$v_j^{n+1} = v_j^n - \mu\, d_{j-1/2}\, v^n - 1/2\, \mu(1-\mu)\gamma_{j-1/2}\, d_{j-1/2}\, v^n$$
$$= (1 - \sigma_{j-1/2})\, v_j^n + \sigma_{j-1/2}\, v_{j-1}^n$$

where

(5.7b) $$\sigma_{j-1/2} = \mu + \frac{1}{2}\mu(1-\mu)\gamma_{j-1/2} \, .$$

We see that the CFL condition $0 < \mu \leq 1$ and (5.6b) imply that

(5.7c) $$0 \leq \sigma_{j-1/2} \leq 1 \, ;$$

thus we conclude

(5.8) $$|d_{j-1/2}\, v^n| \geq \frac{1}{2}\, |D_{j-1/2}\, v^n| \Rightarrow v_j^{n+1} \in [v_{j-1}^n, v_j^n] \, .$$

Relation (5.8) shows that if v^n is monotone for $J_L \leq j \leq J_R$, i.e. $v_{J_L} \leq v_{J_{L+1}} \leq \cdots \leq v_{J_R}$, or $v_{J_L} \geq v_{J_{L+1}} \geq \cdots \geq v_{J_R}$, then v^{n+1} is monotone for $J_L + 1 \leq j \leq J_R$, and in the same sense. Relation (5.8) also shows that mesh-extrema of v^n, i.e. those for which Q has its local extremum at a mesh point, are being damped at the n-th time-step. Namely,

(5.9a) $|d_{j\pm 1/2}\, v^n| \geq \frac{1}{2}\, |D_{j\pm 1/2}\, v^n|,\ v_{j-1}^n \leq v_j^n \geq v_{j+1}^n \Rightarrow \max(v_j^{n+1}, v_{j+1}^{n+1}) \leq v_j^n$

(5.9b) $|d_{j\pm 1/2}\, v^n| \geq \frac{1}{2}\, |D_{j\pm 1/2}\, v^n|,\ v_{j-1}^n \geq v_j^n \leq v_{j+1}^n \Rightarrow \min(v_j^{n+1}, v_{j+1}^{n+1}) \geq v_j^n$.

We turn now to consider interior local extrema of v^n, i.e. those for which

Q has its local extremum in the interior of some (x_i, x_{i+1}). We recall that such an extremum is characterized by $|d_{i+1/2}\, v^n| < 1/2\, |D_{i+1/2}\, v^n|$ and that S_i^n and S_{i+1}^n in this case are given by (4.14); therefore $S_{i+1}^n - S_i^n = D_{i+1/2}\, v^n$. From (5.3a) and (4.6a) we see that in general

(5.10a) $$v_{i+1}^{n+1} - Q(x_{i+1} - a\tau; v^n) = \frac{1}{2}\, \mu(1-\mu)(D_{i+1/2}\, v^n - S_{i+1}^n + S_i^n)\, .$$

Hence

(5.10b) $$|d_{i+1/2}\, v^n| < \frac{1}{2}\, |D_{i+1/2}\, v^n| \Rightarrow v_{i+1}^{n+1} = Q(x_{i+1} - a\tau; v^n)\, .$$

Relation (5.10b) confirms the second order accuracy of the scheme at local extrema. Although it does not necessitate accentuation of the extremal values, as v_{i+1}^{n+1} in (5.10b) may still be in $[v_i^n, v_{i+1}^n]$, it does allow v_{i+1}^{n+1} to deviate from this interval by as much as

(5.10c) $$\frac{1}{2}\, |D_{i+1/2}\, v^n| (|d_{i+1/2}\, v^n| / |D_{i+1/2}\, v^n| - 1/2)^2$$

Thus (5.10b) is the essential difference between the present scheme and the "second order" TVD schemes.

A similar analysis, which we do not present here, shows that if v_i^n is a mesh-extremum then $v_j^{n+1}, j = i, i+1$, relates to $Q(x_j - a\tau; v^n)$ in the following way:

(5.11a) $v_j^{n+1} \geq Q(x_j - a\tau; v^n)$, $j = i, i+1$, if v_i^n is a maximum

(5.11b) $v_j^{n+1} \leq Q(x_j - a\tau; v^n)$, $j = i, i+1$, if v_i^n is a minimum.

From (5.9)-(5.11) we deduce the following relation between the total variation of the numerical solution and that of its piecewise-parabolic interpolant Q:

$$TV(\{Q(x_j - a\tau; v^n)\}) \le TV(v^{n+1}) \le TV(Q(\cdot; v^n)) \ . \tag{5.12}$$

The LHS of (5.12) is the total variation of the mesh function $\{Q(x_j - a\tau; v^n)\}$. Relation (5.12) suggests to consider an equivalent definition $\overline{TV}$ of the total variation of the numerical approximation of the form

$$\overline{TV}(v^n) = TV(Q(\cdot; v^n))$$

with the hope that the scheme (5.3) is TVD with respect to this modified definition. Unfortunately our numerical experiments have shown that there are instances, although rather rare, that $\overline{TV}(v^n)$ is increasing with n; the same is true for $\overline{TV}(v^n) = TV(L(\cdot; v^n))$.

As we have mentioned in the introduction, because of the nonoscillatory nature of the scheme, uniform total variation boundedness of the numerical solution is implied by uniform boundedness of its maximum norm. If we follow a particular local maximum of the initial data we see from (5.9)-(5.10a) that it actually decreases most of the time, and whenever it does increase (5.10c) and (3.10) suggest that it does so by a "small amount" that vanishes with $h \to 0$. Since the initial data is only piecewise-smooth we have not been able as yet to rigorize these arguments.

We remark that our numerical experiments clearly indicate that in a normal computational situation the maximum norm of the numerical solution is indeed uniformly bounded. We feel that our inability to prove this fact stems only from lack of theoretical tools to analyse pointwise regularity of the numerical solution.

6. The nonlinear case. In this section we describe an approximate solution $v_n(x, t)$ of [5] for the IVP (2.2)

$$(6.1) \qquad v_t + f(v)_x = 0, \;\; v(x,0) = L(x; v^n) \,.$$

This approximate solution is consistent with the conservation form of the equation (6.1) in the sense that the cell-averaging (2.3) results in a scheme in conservation form i.e.

$$(6.2) \qquad v_j^{n+1} = \frac{1}{h} \int_{x_{j-1/2}}^{x_{j+1/2}} v_n(x,\tau)\, dx = v_j^n - \lambda(\hat{f}_{j+1/2} - \hat{f}_{j-1/2})$$

where the numerical flux $\hat{f}_{j+1/2}$ is consistent with $f(u)$ in the sense of (1.2c). Furthermore, the approximate solution operator is TVD

$$(6.3) \qquad TV(v_n(\cdot\,; t)) \le TV(v_n(\cdot\,; 0)) = TV(L(\cdot\,; v^n)) \;\; \text{for} \;\; 0 \le t \le \tau$$

and thus by the reasoning presented in section 2, the resulting scheme (6.2) is non-oscillatory.

We turn now to outline the derivation of this approximate solution. To simplify our presentation we ignore entropy considerations and refer the reader to future papers for details of appropriate modifications. We assign to the point $x_{j+1/2}$ a characteristic speed that corresponds to the Rankine-Hugoniot speed $\bar{a}_{j+1/2}$ of the two neighbouring cell-averages v_j^n and v_j^{n+1}

$$(6.4a) \qquad \bar{a}_{j+1/2} = \begin{cases} \dfrac{f(v_{j+1}^n) - f(v_j^n)}{v_{j+1}^n - v_j^n} & \text{if } v_j^n \ne v_{j+1}^n \\ a(v_j^n) & \text{if } v_j^n = v_{j+1}^n \end{cases} ,$$

and denote by $\bar{a}(x)$ the piecewise-linear interpolant of $\{\bar{a}_{j+1/2}\}$, i.e.

(6.4b) $\bar{a}(x) = \bar{a}_{j-1/2} + (\bar{a}_{j+1/2} - \bar{a}_{j-1/2}) \cdot (x - x_{j-1/2})/h$

$$\text{for } x_{j-1/2} \leq x \leq x_{j+1/2} .$$

The approximate solution $v_n(x,t)$ is defined by specifying its constancy along the approximate characteristics

(6.5a)
$$x(t) = x_0 + \bar{a}(x_0) \cdot t$$

i.e.

(6.5b)
$$v_n(x(t), t) \equiv v_n(x_0,0) = L(x_0; v^n) .$$

Using (6.5a) and (6.4b) to express x_0 in terms of x and t

6.5c) $x_0(x,t) = x_{j-1/2} + h \cdot[x - x_{j-1/2}(t)]/[x_{j+1/2}(t) - x_{j-1/2}(t)]$

$$\text{for } x_{j-1/2}(t) < x < x_{j+1/2}(t)$$

we get from (6.5b) that

(6.6a)
$$v_n(x,t) = L\left(x_{j-1/2} + h \cdot \frac{x - x_{j-1/2}(t)}{x_{j+1/2}(t) - x_{j-1/2}(t)};\ v^n\right)$$

$$\text{for } x_{j-1/2}(t) < x < x_{j+1/2}(t)$$

where

(6.6b)
$$x_{i+1/2}(t) = x_{i+1/2} + t \cdot \bar{a}_{i+1/2} .$$

Taking cell-averages of the approximate solution (6.6) we get the conservation form (6.2)

(6.7a)
$$v_j^{n+1} = v_j^n - \lambda(\hat{f}_{j+1/2} - \hat{f}_{j-1/2})$$

with the numerical flux

$$\text{(6.7b)} \qquad \hat{f}_{j+1/2} = \begin{cases} f(v_j^n) + 1/2\ \bar{a}_{j+1/2}\,(1 - \lambda\ \bar{a}_{j-1/2}) \cdot \hat{S}_j & \text{if } \bar{a}_{j+1/2} \geq 0 \\ f(v_{j+1}^n) - 1/2\ \bar{a}_{j+1/2}(1 + \lambda\ \bar{a}_{j+3/2}) \cdot \hat{S}_{j+1} & \text{if } \bar{a}_{j+1/2} \leq 0 \end{cases},$$

where

$$\text{(6.7c)} \qquad \hat{S}_j = S_j^n/[1 + \lambda(\bar{a}_{j+1/2} - \bar{a}_{j-1/2})]\ .$$

Note that (6.7) is identical to (5.30) in the constant coefficient case.

We turn now to prove that the scheme (6.7) is uniformly second-order accurate in the sense of (2.9). Starting with the exact cell-averages $v_j^n = \bar{u}_j^n$ in (6.7) this amounts to showing that

$$\text{(6.8a)} \qquad \hat{f}_{j+1/2} = \hat{f}_{j+1/2}(u) + O(h^2)$$

with a sufficiently smooth coefficient in the $O(h^2)$ term; here $\hat{f}_{j+1/2}$ is the numerical flux (6.7b) computed with the exact cell-averages, and $\hat{f}_{j+1/2}(u)$ is (2.1b). We shall do so in two steps: first we shall show that

$$\text{(6.8b)} \ \hat{f}_{j+1/2}(u) = \frac{1}{2}[f(L(x_{j+1/2};\ \bar{u}^n)) + f(L(x_0(x_{j+1/2}, \tau); \bar{u}^n))] + O(h^2)\ ,$$

where $x_0(x_{j+1/2},\tau)$ is (6.5c), and then we shall verify that

$$\text{(6.8c)} \qquad \frac{1}{2}[f(L(x_{j+1/2}; \bar{u}^n)) + f(L(x_0(x_{j+1/2}, \tau); \bar{u}^n))] = \hat{f}_{j+1/2} + O(h^2)\ .$$

Special attention will be given to the smoothness of the $O(h^2)$ coefficients.

To show (6.8b) we start by using the trapezoidal rule to approximate the integral in (2.1b); we get

$$\text{(6.9a)} \qquad \hat{f}_{j+1/2}(u) = \frac{1}{2}[f(u(x_{j+1/2}, t_n)) + f(u(x_{j+1/2}, t_n + \tau))] + O(h^2)\ .$$

The smoothness of the $O(h^2)$ term follows from that of $f(u)$ and $u(x,t)$. Next we observe that $\bar{a}(x)$ in (6.4b) approximates $a(u(x,t_n))$ to $O(h^2)$, and therefore we can use the approximate characteristic line (6.5c) to trace $u(x_{j+1/2}, t_n + \tau)$ to $u(x_0(x_{j+1/2}, \tau), t_n)$ with $O(h^3)$ accuracy; consequently

(6.9b) $$f(u(x_{j+1/2}, t_n + \tau)) = f(u(x_0(x_{j+1/2}, \tau), t_n)) + O(h^3) .$$

Finally we obtain (6.8b) by approximating $u(x,t_n)$ in (6.9a) and (6.9b) to $O(h^2)$ by $L(x; \bar{u}^n)$ (see (4.4)). The smoothness of the $O(h^2)$ term in this approximation is due to (4.4c):

$$S_j^n = h \cdot u_x(x, t_n) + O(h^3) .$$

(We recall that the degeneracy to first order accuracy at local extrema points of some "second-order accurate" TVD schemes is due to lack of smoothness there of the $O(h^2)$ term in (2.7a)).

We turn now to verify (6.8c). First let us consider the case $\bar{a}_{j+1/2} \geq 0$:

$$L(x_{j+1/2}; \bar{u}^n) = \bar{u}_j^n + \frac{1}{2} S_j^n ,$$

$$L(x_0(x_{j+1/2}, \tau); \bar{u}^n) = \bar{u}_j^n + \left[\frac{1}{2} - \frac{\lambda \bar{a}_{j+1/2}}{1 + \lambda(\bar{a}_{j+1/2} - \bar{a}_{j-1/2})}\right] S_j^n ,$$

and expand the LHS of (6.8c) around $\bar{u}_j^n$. We get

(6.10a) $$f(\bar{u}_j^n) + \frac{1}{2} a(\bar{u}_j^n)(1 - \lambda\, \bar{a}_{j+1/2})\, \hat{S}_j + \frac{1}{8} a'(\bar{u}_j^n)[(1 - \lambda\, \bar{a}_{j-1/2})^2$$

$$+ (\lambda \bar{a}_{j+1/2})^2](\hat{S}_j)^2 + O(h^3) = \hat{f}_{j+1/2} + \frac{h^2}{8}(2\lambda^2 a^2 - 1) \cdot a' \cdot (u_x)^2|_{j+1/2} + O(h^3) .$$

Similarly in the case $\bar{a}_{j+1/2} \leq 0$:

$$L(x_{j+1/2}; \bar{u}^n) = \bar{u}_{j+1} - \frac{1}{2} S^n_{j+1}, \quad L(x_0(x_{j+1/2}, \tau); \bar{u}^n)$$

$$= \bar{u}^n_{j+1} - \left[\frac{1}{2} + \frac{\lambda \bar{a}_{j+1/2}}{1 + \lambda(\bar{a}_{j+3/2} - \bar{a}_{j+1/2})}\right] \cdot S^n_{j+1} ,$$

we expand the LHS of (6.8c) around $\bar{u}^n_{j+1}$ to get

$$(6.10b) f(\bar{u}^n_{j+1}) - \frac{1}{2} a(\bar{u}^n_{j+1})(1 + \lambda \bar{a}_{j+3/2})\hat{S}_{j+1}$$

$$+ \frac{1}{8} a'(u^n_{j+1})[(1 + \lambda \bar{a}_{j+3/2})^2 + (\lambda \bar{a}_{j+1/2})^2] \cdot (\hat{S}_{j+1})^2 + O(h^3)$$

$$= \hat{f}_{j+1/2} + \frac{h^2}{8} (2\lambda^2 a^2 - 1) \cdot a' \cdot (u_x)^2|_{j+1/2} + O(h^3) .$$

We see from (6.10a) and (6.10b) that independently of the sign of $\bar{a}_{j+1/2}$, the $0(h^2)$ term in (6.8c) is the same, namely

$$\frac{h^2}{8} (2\lambda^2 a^2 - 1) \cdot a' \cdot (u_x)^2|_{j+1/2} .$$

This completes the proof that the scheme (6.7) is second-order accurate in the sense of (2.9) wherever $u(x,t)$ is smooth, including local extrema and sonic $(f' = 0)$ points.

Remarks: (1) The numerical flux (6.7b) can be rewritten as:

$$(6.11) \quad \hat{f}_{j+1/2} = \frac{1}{2} \Big[f(v^n_j) + f(v^n_{j+1}) - |\bar{a}_{j+1/2}| (v^n_{j+1} - v^n_j)$$

$$+ \max(0, \bar{a}_{j+1/2}) \cdot (1 - \lambda \bar{a}_{j-1/2}) \cdot \hat{S}_j$$

$$- \min(0, \bar{a}_{j+1/2}) \cdot (1 + \lambda \bar{a}_{j+3/2}) \cdot \hat{S}_{j+1} \Big] .$$

(2) Our proof that the scheme (6.7) is non-oscillatory is based on the representation of (6.7) as the cell-average (6.2) of the non-oscillatory approximate solution $v_n(x,t)$ in (6.6). To ensure that $v_n(x,t)$ remains univalued for $0 \le t \le \tau$ we have to restrict the time-step τ so that for all j

(6.12a) $$x_{j+1/2}(\tau) > x_{j-1/2}(\tau) .$$

This implies the condition

(6.12b) $$\tau \max_j(\bar{a}_{j-1/2} - \bar{a}_{j+1/2}) \le h .$$

On the other hand, to derive the particular form of the numerical flux (6.7b) we have made the assumption

(6.13a) $$|x_{j+1/2}(\tau) - x_{j+1/2}| < h \text{ for all } j ,$$

which implies the condition.

(6.13b) $$\tau \max_j|\bar{a}_{j+1/2}| < h .$$

The two time-step restrictions (6.12b) and (6.13b) are characteristic to Godunov-type schemes. The practice of reconciling the two conditions by

$$\tau \max_j|\bar{a}_{j+1/2}| \le h/2$$

is completely unnecessary: The scheme (6.7), as the original Godunov scheme, remains non-oscillatory (or TVD in the case analysed in [10]) for the full CFL-restriction (6.13b). The reasoning for this observation is as follows: The approximate solution (6.6) under the CFL restriction (6.13b) may fail to be univalued in the j-th cell only if $\bar{a}_{j-1/2} > 0$ and $\bar{a}_{j+1/2} < 0$. In this case the numerical fluxes $\hat{f}_{j\pm1/2}$ as defined by cell-averaging in the neighboring cells $j \pm 1$, remain (6.7b). Thus the only thing that needs to be changed in this case is the definition of

$v_n(x,\tau)$ in the j-th cell.

(3) We observe that once $v_n(x,\tau)$ is defined globally in (6.6) there is no intrinsic need to average it on the original mesh. We may average it on different intervals and still conclude that the resulting approximation is non-oscillatory and conservative. Furthermore, the construction of the interpolant Q, the approximation L and the approximate characteristic field $\bar{a}(x)$ needed to define $v_n(x, t)$, does not depend on the uniformity of the mesh. Therefore the scheme (6.7) generalizes immediately to non-uniform moving meshes. Of particular computational interest are the self-adjusting moving grids of the type described in [12], which make it possible to obtain perfectly resolved shocks and contact discontinuities.

(4) We note that since the approximate solution $v_n(x,t)$ in (6.6) is conservative, it is possible to consider an associated random-choice method obtained by replacing the cell-averaging in (6.2) by a sampling with respect to a variable that is uniformly distributed in the cell, i.e.

$$v_j^{n+1} = v_n(x_j + \theta_j^n h, \tau)$$

where θ_j^n is uniformly distributed in $[-1/2, 1/2]$. Following the reasoning of [7] it is clear that the resulting random-choice method is non-oscillatory and that its limits are weak solutions of (1.1). Although the random-choice approach has many attractive computational features, it has been our experience that in many application it is possible to accomplish the same computational goals with a self-adjusting moving grid. In this case the use of the latter is preferable as it offers gain in resolution without a loss in pointwise accuracy that is associated with sampling.

7. Numerical Illustration. In this section we compare the new uniformly second-order non-oscillatory scheme of this paper (to be refered to as UN02) to the typical second-order TVD scheme (to be refered to as TVD2). Both schemes can be written in the form (6.7), i.e.

$$v_j^{n+1} = v_j^n - \lambda(\hat{f}_{j+1/2} - \hat{f}_{j-1/2}) , \tag{7.1a}$$

$$\hat{f}_{j+1/2} = \begin{cases} f(v_j^n) + 1/2\, \bar{a}_{j+1/2}(1 - \lambda\bar{a}_{j-1/2})S_j^n/[1 + \lambda(\bar{a}_{j+1/2} - \bar{a}_{j-1/2})] \\ \qquad \text{if } \bar{a}_{j+1/2} \geq 0 \\ f(v_{j+1}^n) - 1/2\, \bar{a}_{j+1/2}(1 + \lambda\bar{a}_{j+3/2})S_{j+1}^n/[1 + \lambda(\bar{a}_{j+3/2} - \bar{a}_{j+1/2})] \\ \qquad \text{if } \bar{a}_{j+1/2} \leq 0 \end{cases} \tag{7.1b}$$

$$S_j^n = m(S_j^+, S_j^-); \tag{7.1c}$$

here $\bar{a}_{j+1/2}$ is (6.4a) and $m(x,y)$ is the min mod function (3.3). $S_j^{\pm}$ are different for TVD2 and UN02:

$$\text{TVD2:}\ S_j^{\pm} = d_{j\pm 1/2}v^n \tag{7.2}$$

$$\text{UNO2:}\ S_j^{\pm} = d_{j\pm 1/2}v^n \mp \frac{1}{2} D_{j\pm 1/2}v^n , \tag{7.3}$$

where $d_{i+1/2}$ and $D_{i+1/2}$ are defined in (3.2).

UNO2 and TVD2 are both second-order accurate Godunov-type schemes that differ only in the reconstruction step (4.2a):

$$L(x;u) = u_j + S_j(x - x_j)/h \ \text{ for } \ |x - x_j| < h/2 , \tag{7.4a}$$

where the slopes of the lines are calculated by (7.3) and (7.2), respectively. Therefore we start our comparison on the approximation level.

In Table 1 and Fig. 1 we present approximations to

$u(x) = \sin\pi x$, $-1 \leq x \leq 1$. We divide $[-1,1]$ into N equal intervals and define

(7.4b) $$x_j = -1 + j \cdot \frac{2}{N}, \quad 0 \leq j \leq N .$$

The symbols in Fig. 1 denotes values of $u_j = \sin\pi x_j$ for $N = 10$ in (7.4b). In Fig. 1a we show the piecewise-parabolic interpolant $Q(x;u)$ (see section 3). In Fig. 1b we show the piecewise-linear approximation $L^{\text{UN02}}(x;u)$ which is (7.4a) with (7.1c) and (7.3). In Fig. 1c we show the piecewise-linear approximation $L^{\text{TVD2}}(x;u)$ which is (7.4a) with (7.1c) and (7.2). We make the following observations regarding Fig. 1: (i) Q is a better approximation than L^{UN02}; L^{UN02} is a better approximation than L^{TVD2}. (ii) $TV(L^{\text{UN02}}) > TV(u) > TV(L^{\text{TVD2}})$. In table 1 we quantify the first observation; we list the L_∞-error and the L_1-error of these approximations to $\sin\pi x$ for a refinement sequence of $N = 10,20,40,80$ in (7.4b). Clearly Q is an $O(h^3)$ approximation, while L^{UN02} and L^{TVD2} are $O(h^2)$. The error in L^{UN02} is about a 1/3 of the error in L^{TVD2}.

In Table 2 and Fig. 2 we present solutions of UN02 and TVD2 for the constant coefficient case

(7.6) $$u_t + u_x = 0, \;\; u(x,0) = \sin \pi x, \;\; -1 \leq x \leq 1$$

with periodic boundary conditions, at $t = 2$ with $\tau/h = 0.8$. Figs 3a and 3b show UN02 and TVD2, respectively, with $N = 20$ in (7.4b). In table 2 we list the L_∞-error and L_1-error for a refinement sequence with $N = 20,40,80,160$. Clearly UN02 is second-order accurate in both L_∞ and L_1, while TVD2 is second-order accurate in L_1 but only first order accurate in L_∞. Fig. 3b demonstrates that the degeneracy to first order accuracy at local extrema in the TVD scheme adversely affects the accuracy everywhere (Because the scheme is TVD it cannot switch abruptly to second-order accuracy as this would introduce oscillatious; consequently it takes quite a while to recover the second order accuracy).

Next we approximate the discontinuous function

$$u(x) = \begin{cases} -x\sin(3\pi x^2/2) \ , & -1 < x < -1/3 \\ |\sin(2\pi x)| \ , & |x| < 1/3 \\ 2x - 1 - 1/6\sin(3\pi x) \ , & 1/3 < x < 1 \end{cases} \tag{7.7}$$

which we extend to have period 2 outside $[-1,1]$.

In Fig 3 we present approximations to $\phi(x)$, using $N = 20$. Fig 3a shows $Q(x;\bar{u})$, Fig 3b shows $L^{UN02}(x;\bar{u})$, and Fig 3c shows $L^{TVD2}(x;\bar{u})$. We again observe that Q is better approximation then L^{UN02}, while L^{UN02} is a better approximation then L^{TVD2}.

In Fig 4 we present solutions of $UN02$ and $TVD2$ for the constant coefficient problem (7.6), initial data given by (7.2), and periodic boundary conditions. We take $t = 2$ and $\tau/h = 0.8$. Figs 4a and 4b show UN02 and TVD2 respectively with $N = 40$. Fig 4b shows the damping effect that the TVD scheme imposes due to its degeneracy to first order accuracy at local extrema.

In Fig 5 we solve the same problems, except we impose boundary conditions. At $x = -1$ we impose the given function (7.7) evaluated at $-1 - t$. No boundary conditions are imposed at $x = 1$. We implement this numerically using UN02 and TVD2 except at the boundary points. There we are in general, unable to construct non-oscillatory piecewise parabolic interpolants $Q(x,\bar{u})$, so we construct the only possible parabolic interpolant thru x_i, x_{i+1} and the point to either the left or right which lies in the region. The analogous procedure is carried out at the reconstruction stage. Figs 5a and 5b again show the results at $t = 2$ with $\tau/h = 0.8$.

The possible introduction of oscillations through the boundary conditions does not seem to have degraded the performance of either scheme (in fact the opposite is observed). Again the TVD2 scheme shows a damping effect.

In Table 3 and Fig. 6 we present results for Burgers' equation

$$(7.8) \qquad u_t + uu_x = 0, \; u(x,0) = \alpha + \sin \pi(x + \beta), \; -1 \leq x \leq 1$$

with periodic boundary conditions and $\tau/h\,(1 + |\alpha|) = 0.5$. The solution to (7.7) is smooth for $t < 1/\pi$; at $t = 1/\pi$ it develops shocks. In Table 3a we list the L_∞-error and L_1-error of UN02 and TVD2 at $t = 0.15$ for $\alpha = \beta = 0$ in (7.7). This table shows the same asymptotic behaviour as Table 2, except that because of the large gradients it shows for a smaller h.

In Figs 6a and 6b we show results of UN02 and TVD2 for (7.8) with $\alpha = 2$ and $\beta = 1$ at $t = 0.35$ with $N = 20$. In this case the solution to (7.8) develops a shock moving with speed 2 beginning at time $t = 1/\pi \approx 0.318$.

In Table 3b and Figs 6c and 6d we repeat the previous calculations for the schemes (2.13):

$$(7.9a) \qquad v_j^{n+1} = v_j^n - \lambda(\hat{f}_{j+1/2} - \hat{f}_{j-1/2})$$

$$(7.9b) \qquad \hat{f}_{j+1/2} = f(v_n(x_{j+1/2}, \tau/2)) = f(L(x_0(x_{j+1/2}, \tau/2), v^n))$$

where $x_0(x_{j+1/2}, \tau/2)$ is (6.5c), i.e.

$$(7.9c) \quad \hat{f}_{j+1/2} = \begin{cases} f\left(v_j^n + \dfrac{1}{2} \cdot \dfrac{1 - \lambda(\hat{a}_{j+1/2} + \hat{a}_{j-1/2})/2}{1 + \lambda(\hat{a}_{j+1/2} - \hat{a}_{j-1/2})/2} \cdot S_j^n\right) & \text{if } \hat{a}_{j+1/2} \geq 0 \\ f\left(v_{j+1}^n - \dfrac{1}{2} \cdot \dfrac{1 + \lambda(\hat{a}_{j+3/2} + \hat{a}_{j+1/2})/2}{1 + \lambda(\hat{a}_{j+3/2} - \hat{a}_{j+1/2})/2} \cdot S_{j+1}^n\right) & \text{if } \hat{a}_{j+1/2} \leq 0 \end{cases}$$

As we have remarked in section 2, v_j^{n+1} in (7.9a) is not a cell-average of $v_n(x,\tau)$, but only an approximation to it. Therefore it is not necessary to take $\hat{a}_{j+1/2}$ in (7.8c) to be (6.4a). We choose $\hat{a}_{j+1/2}$ so that (7.9c) is continuous at $\hat{a}_{j+1/2} = 0$:

$$(7.9\text{d})\ \hat{a}_{j+1/2} = \left[f(v_{j+1}^n - \frac{1}{2}S_{j+1}^n) - f(v_j^n + \frac{1}{2}S_j^n) \right] / \left[(v_{j+1}^n - \frac{1}{2}S_{j+1}^n) - (v_j^n + \frac{1}{2}S_j^n) \right] .$$

We denote the schemes (7.9) with S_j^n defined by (7.1c) and either (7.2) or (7.3) by FVD2 and FN02, respectively. We note that (7.9) is identical to (7.1) in the constant coefficient case, and consequently FVD2 and FN02 are nonoscillatory in the constant coefficient case. Figs 6c and 6d show that FN02 and FVD2 are also non oscillatory in the case (7.8). Furthermore, Table 3b shows that FN02 is much more accurate than UN02 (FVD2 is about the same as TVD2).

In all previous examples we have presented pointwise calculations; namely, we have initialized the numerical solution by taking v_j^0 to be the value of the initial data at x_j, and we have considered v_j^n to be an approximation to $u(x_j,t_n)$. (Surely this is an acceptable practice for second order accurate schemes.) In Table 3c we repeat the calculation for UN02 in Table 3a, but now in a sense of cell-averages and denote it by AN02. Now we initialize UN02 for (7.8) with $\alpha = \beta = 0$ by cell-averages of the initial data, i.e.

$$(7.10\text{a})\ v_j^0 = -\frac{1}{\pi h}\left[\cos(\pi x_{j+1/2}) - \cos(\pi x_{j-1/2})\right] = \frac{\sin(\pi h/2)}{(\pi h/2)} \cdot \sin(\pi x_j) ,$$

and regard v_j^n to represent cell-averages of $u(x,t_n)$. To obtain a pointwise approximation to $u(x,t_n)$ we first compute point values $V_{j+1/2}^n$ of its indefinite integral $u^n(x_{j+1/2}) = \int_{x_0}^{x_{j+1/2}} u(y,t_n)\, dy$ by

(7.10b)
$$V_{j+1/2}^n = h \sum_{i=i_0}^{j} v_i^n .$$

Next we obtain a global piecewise-linear approximation $v(x,t_n)$ to $u(x,t_n)$ by

(7.10c)
$$v(x,t_n) = \frac{d}{dx} Q(x;V^n)$$

where Q is the piecewise-parabolic interpolant of section 3. Finally we get

(7.10d)
$$v(x_j,t_n) = \frac{d}{dx} Q(x_j;V^n) = \frac{1}{h}(V_{j+1/2}^n - V_{j-1/2}^n) = v_j^n .$$

Thus the only difference between AN02 in Table 3c, and UN02 in Table 3a is the initialization (7.10a), which itself differs only slightly from the mesh values of the initial data (since $\sin(\pi h/2)/(\pi h/2) = 1 - 1/6(\pi h/2)^2 + O(h^4)$).

We remark that cell-averages do play a significant role when the initial data is discontinuous (since they provide information about the location of the discontinuity) and in higher-order Godunov-type schemes; this will be described elsewhere.

We turn now to present calculations with a formal extension of UN02 and TVD2 for systems of conservation laws. We consider a Riemann problem for the Euler equations of gas dynamics

(7.11a)
$$u_t + f(u)_x = 0, \quad u(x,0) = \begin{cases} u_L & x < 0 \\ u_R & x > 0 \end{cases},$$

(7.11b)
$$u = (\rho,m,E)^T, f(u) = (m, m^2/\rho + P, m(E+P)/\rho)^T ,$$

(7.11c)
$$P = (\gamma - 1)(E - \frac{1}{2} m^2/\rho) .$$

Here ρ, m, E and P are the density, momentum, total energy and pressure, respectively; we take $\gamma = 1.4$.

In the following we apply the extension technique of [3] to UN02 and TVD2. The idea is to extend UN02 and TVD2 to systems in such a way that will be identical to (7.1) in the scalar case, and will decouple into (5.3) for each of the characteristic variables in the constant coefficient system case. To accomplish that we use Roe's averaging for (7.11) (see [13])

$$v_{j+1/2} = V(v_j^n, v_{j+1}^n) \tag{7.12a}$$

for which

$$f(v_{j+1}^n) - f(v_j^n) = A(v_{j+1/2})(v_{j+1}^n - v_j^n), \quad A(u) = \partial f/\partial u , \tag{7.12b}$$

and define local characteristic variables with respect to the right-eigenvector system $\{R_{j+1/2}^k\}_{k=1}^3$ of $A(v_{j+1/2})$. We extend (6.11) to systems as follows:

$$v_j^{n+1} = v_j^n - \lambda(\hat{f}_{j+1/2} - \hat{f}_{j-1/2}) \tag{7.13a}$$

$$\hat{f}_{j+1/2} = \frac{1}{2}\left[f(v_j^n) + f(v_{j+1}^n) - \sum_{k=1}^{3} c_{j+1/2}^k R_{j+1/2}^k\right] \tag{7.13b}$$

$$\begin{aligned} c_{j+1/2}^k = {} & |\bar{a}_{j+1/2}^k| d_{j+1/2}^k w - \max(0,\bar{a}_{j+1/2}^k)(1 - \lambda\bar{a}_{j-1/2}^k)\hat{S}_j^k \\ & + \min(0,\bar{a}_{j+1/2}^k)(1 + \lambda\bar{a}_{j+3/2}^k)\hat{S}_{j+1}^k . \end{aligned} \tag{7.13c}$$

Here $\bar{a}_{j+1/2}^k$ is the k-th eigenvalue of $A(v_{j+1/2})$ corresponding to $R_{j+1/2}^k$, and $d_{j+1/2}^k w$ denotes the component of $d_{j+1/2}v = v_{j+1}^n - v_j^n$ in the k-th characteristic field, i.e.

$$d_{j+1/2}v = \sum_{k=1}^{3} (d_{j+1/2}^k w)R_{j+1/2}^k . \tag{7.13d}$$

Likewise $\hat{S}_j^k$ denotes the component of the vector of slopes in the k-th characteristic field, and is defined as follows:

(7.13e) $$\hat{S}_j^k = m(S_{-,j}^k, S_{+,j}^k)/[1 + \lambda(\bar{a}_{j+1/2}^k - \bar{a}_{j-1/2}^k)] ;$$

$m(x,y)$ is the min mod function (3.3). $S_{\pm,j}^k$ are different for VD2 and N02:

(7.14) TVD2: $S_{\pm j}^k = d_{j\pm 1/2}^k w$

(7.15) UN02: $S_{\pm,j}^k = d_{j+1/2}^k w \mp \frac{1}{2} D_{j\pm 1/2}^k w$;

$$D_{i\pm 1/2}^k w = m(d_{i+3/2}^k w - d_{i+1/2}^k w,\ d_{i+1/2}^k w - d_{i-1/2}^k w) .$$

In Figs 7.8 and 7.9 we show numerical solutions of UN02 and TVD2, respectively, for the Riemann problem (7.1b) with

$$U_L = (1,0,2.5)^T, \quad U_R = (0.125,0,0.25) .$$

These figures demonstrate that the formal extension to systems is nonoscillatory in this case. Since the solution to the Riemann problem is just constant states seperated by waves we do not get to see here the extra resolution power of UN02, except that its numerical solution is somewhat "crisper" than that of TVD2. In this calculation we have not employed any artificial compression in the linearly degenerate field and therefore the contact discontinuity smears like $n^{1/3}$, as expected. The interested reader is referred to [4], [5] and [10] for a detailed description of such compression techniques, as well as for details of entropy enforcement mechanisms.

References

[1] S.R. Chakravarthy and S. Osher, "A new class of High Accuracy TVD Schemes for Hyperbolic Conservation Laws," AIAA paper 85-0363, Reno, NA. (1985).

[2] P. Colella and P.R. Woodward, The piecewise-parabolic method (PPM) for gas-dynamical simulations, J. Comp. Phys. v. 54, 174-201 (1984).

[3] A. Harten, On a class of High Resoluiton Total-Variation-Stable Finite-Difference Schemes, SINUM, v. 21, pp. 1-23 (1984).

[4] A. Harten, High resolution schemes for hyperbolic consevation laws, J. Comp. Phys., 49(1983), pp. 357-393.

[5] A. Harten, "On second order accurate Godunov-type schemes". to appear.

[6] A. Harten and J.M. Hyman, "A Self-Adjusting Grid for the Computation of Weak Solutions of Hyperbolic Conservation Laws", J. Comp. Phys. v. 50 (1983), pp. 235-269.

[7] A. Harten and P.D. Lax, "A Random Choice finite difference scheme for hyperbolic conservation laws", SINUM, v. 18, (1981), 289-315.

[8] A. Jameson and P.D. Lax, "Conditions for the Construction of Multi-point Total Variation Diminishing Difference Schemes.", Princeton U. MAE Report 1650 (1984).

[9] S. Osher, Convergence of Generalized MUSCL Schemes, NASA Langley Contractor Report 172306, (1984), SINUM (to appear).

[10] S. Osher and S.R. Chakravarthy, "High-resolution schemes and the entropy condition", SINUM, v. 21, (1984), pp. 955-984.

[11] S. Osher and S.R. Chakravarthy, "Very high order accurate TVD schemes", ICASE Report #84-44, (1984).

[12] S. Osher and E. Tadmor, "On the convergence of difference approximations to conservation laws", submitted to Math-Comp.

[13] P.L. Roe, Approximate Riemann solvers, parameter vectors, and difference schemes, J. Comp. Phys., v. 43 (1981), pp. 357-372.

[14] P.K. Sweby, "High resolution schemes using flux limiters for hyperbolic conservation laws, SINUM, v. 21, (1984), pp. 995-1011.

[15] B. Van Leer, Towards the ultimate conservative scheme, II. Monotonicity and conservation combined in a second order scheme, J. Comp. Phys. 14(1974), pp. 361-376.

[16] B. Van Leer, Towards the ultimate conservative difference scheme, IV. A new approach to numerical convection, J. Comp. Phys., 23(1977), pp. 276-298.

Table 1: Approximations to $u(x) = \sin(\pi x)$, $-1 \le x \le 1$, with periodic boundary conditions.

	L_∞-ERROR			L_1-ERROR		
N	Q	L_{UN02}	L_{TVD2}	Q	L_{UN02}	L_{TVD2}
10	1.545×10^{-2}	5.122×10^{-2}	1.420×10^{-1}	1.494×10^{-2}	2.467×10^{-2}	7.016×10^{-2}
20	1.971×10^{-3}	1.231×10^{-2}	3.558×10^{-2}	1.802×10^{-3}	5.576×10^{-3}	1.525×10^{-2}
40	2.476×10^{-4}	3.083×10^{-3}	9.163×10^{-3}	2.148×10^{-4}	1.355×10^{-3}	3.902×10^{-3}
80	3.104×10^{-5}	7.710×10^{-4}	2.308×10^{-3}	2.617×10^{-5}	3.351×10^{-4}	9.787×10^{-4}

Table 2: Numerical solutions of $u_t + u_x = 0$, $u(x,0) = \sin \pi x$, $-1 \le x \le 1$ at $t = 2$ with periodic boundary conditions and $\tau/h = 0.8$.

	L_∞-ERROR		L_1-ERROR	
N	UN02	TVD2	UN02	TVD2
20	7.097×10^{-3}	8.119×10^{-2}	8.944×10^{-3}	6.778×10^{-2}
40	1.607×10^{-3}	3.477×10^{-2}	2.044×10^{-3}	2.033×10^{-2}
80	3.870×10^{-4}	1.453×10^{-2}	4.926×10^{-4}	5.626×10^{-3}
160	9.201×10^{-5}	5.975×10^{-3}	1.172×10^{-4}	1.528×10^{-3}

Table 3a. Numerical solutions of $u_t + uu_x = 0$, $u(x,0) = \sin\pi x$, at $t = 0.15$ and $\tau/h = 0.5$ – UNO2 and TVD2

	L_∞-ERROR		L_1-ERROR	
N	UN02	TVD2	UN02	TVD2
20	1.890×10^{-2}	2.238×10^{-2}	1.090×10^{-2}	1.854×10^{-2}
40	5.712×10^{-3}	1.054×10^{-2}	3.034×10^{-3}	5.051×10^{-3}
80	1.552×10^{-3}	4.422×10^{-3}	7.771×10^{-4}	1.340×10^{-3}
160	3.985×10^{-4}	1.837×10^{-3}	1.965×10^{-4}	3.621×10^{-4}

Table 3b. Same as Table 3a for FN02 and FVD2.

	L_∞-ERROR		L_1-ERROR	
N	FN02	FVD2	FN02	FVD2
20	6.938×10^{-3}	2.091×10^{-2}	3.726×10^{-3}	1.322×10^{-2}
40	1.959×10^{-3}	1.054×10^{-2}	8.869×10^{-4}	3.835×10^{-3}
80	5.106×10^{-4}	4.424×10^{-3}	2.163×10^{-4}	1.072×10^{-3}
160	1.251×10^{-4}	1.837×10^{-3}	5.270×10^{-5}	2.946×10^{-4}

Table 3c. Same as table 3a for AN02.

N	L_∞-ERROR	L_1-ERROR
20	2.249×10^{-2}	1.221×10^{-2}
40	6.623×10^{-3}	3.243×10^{-3}
80	1.781×10^{-3}	8.259×10^{-4}
160	4.597×10^{-4}	2.079×10^{-4}

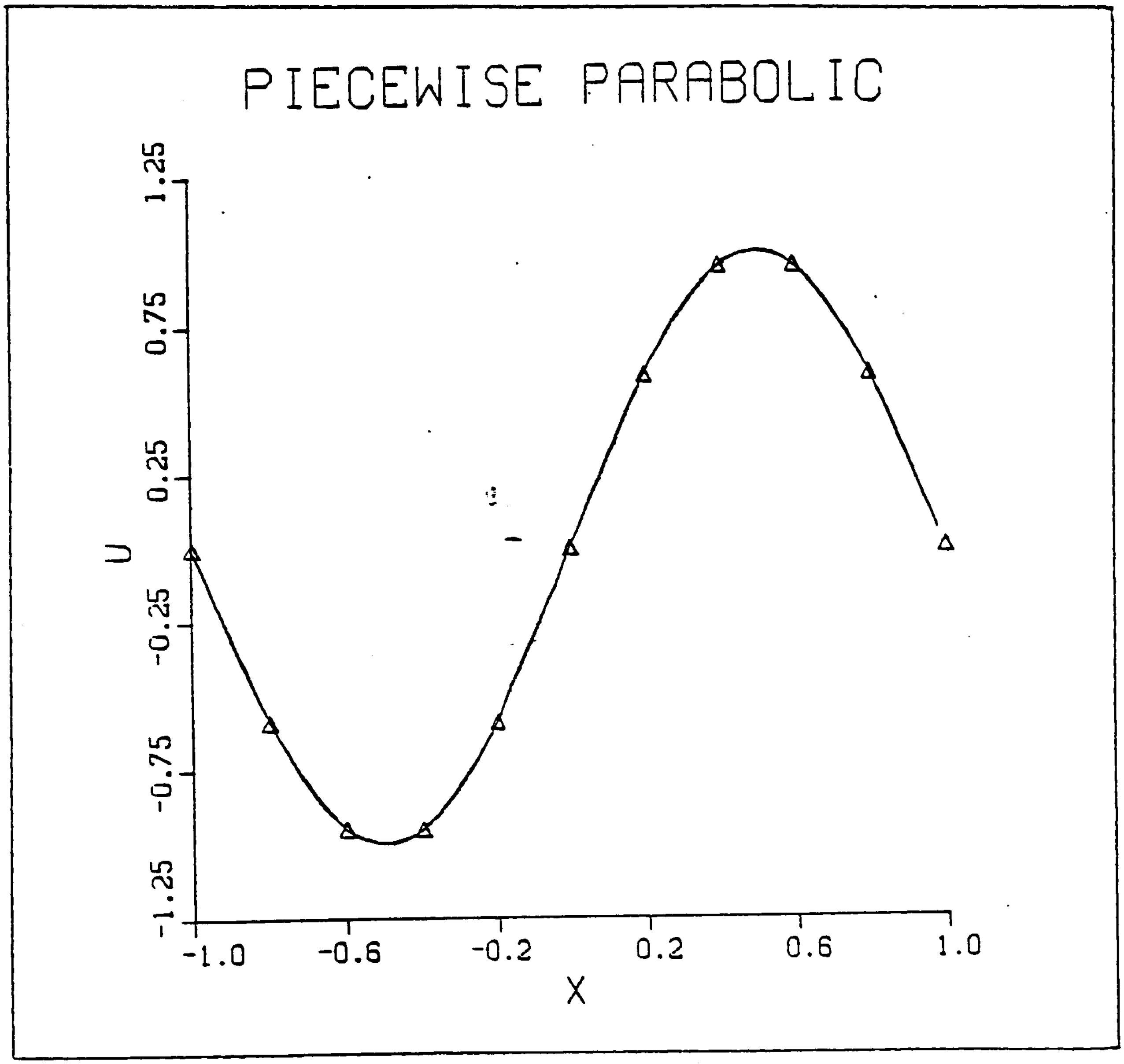

Figure 1a

Figure 1. Approximations of $u = \sin \pi x$, $-1 \le x \ge 1$, with $N = 10$.
a) Piecewise-Parabolic interpolant $Q(\lambda, u)$.

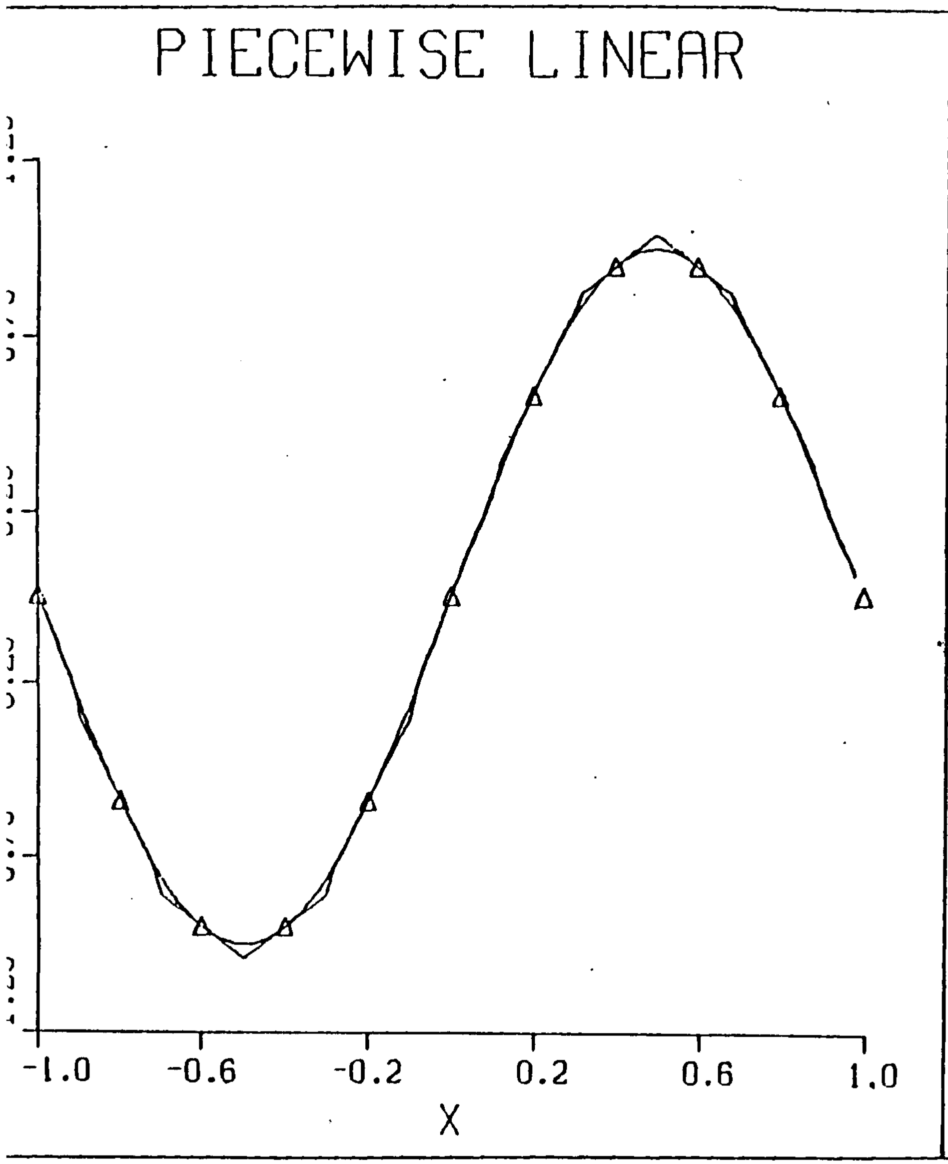

Figure 1b

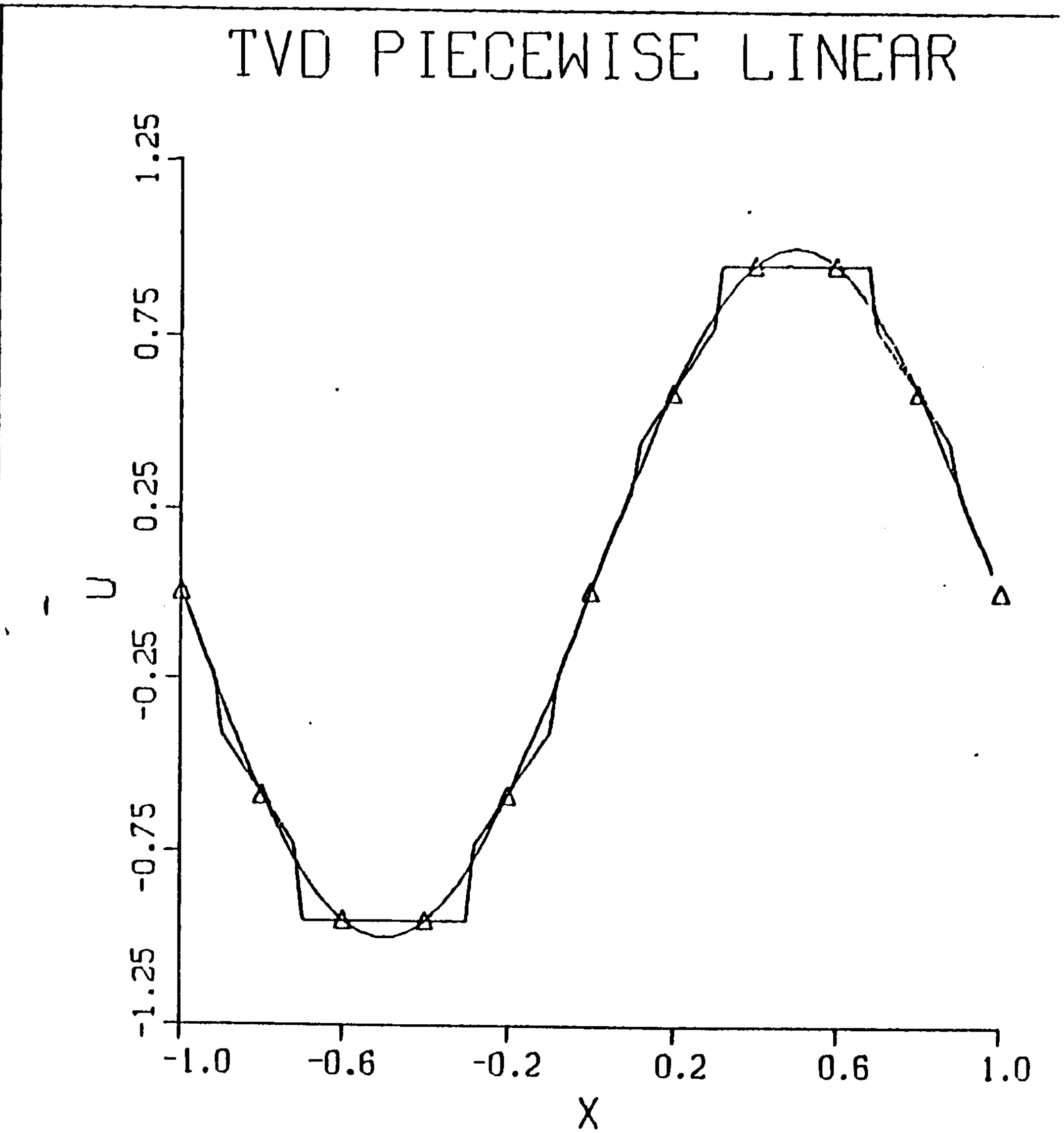

Figure 1c

Figure 1. Approximations of $u = \sin \pi x$, $-1 \le x \le 1$ with $N = 10$.

(b) Piecewise-linear approximation $L^{UNO2}(x;u)$.

(c) Piecewise-linear approximation $L^{TVD2}(x;u)$.

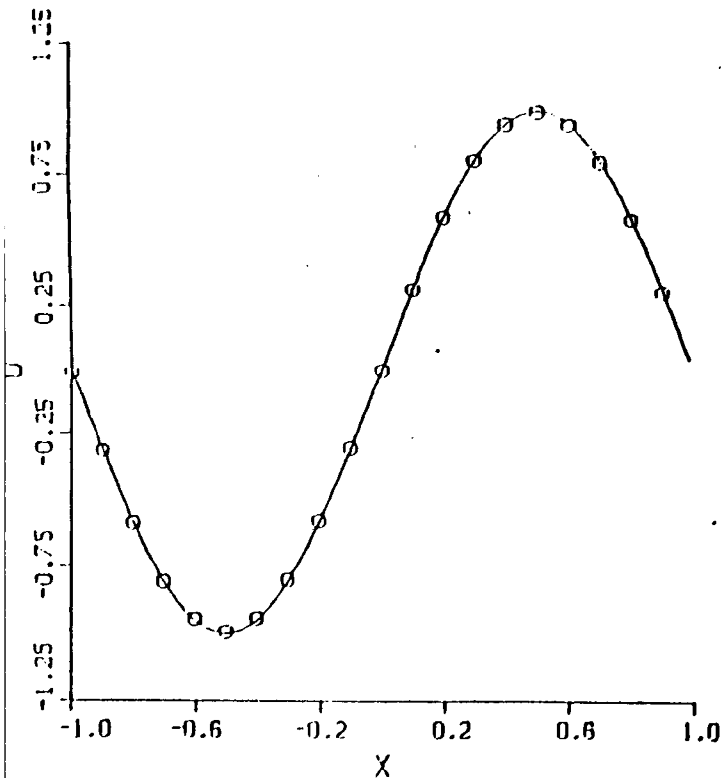

Figure 2a.

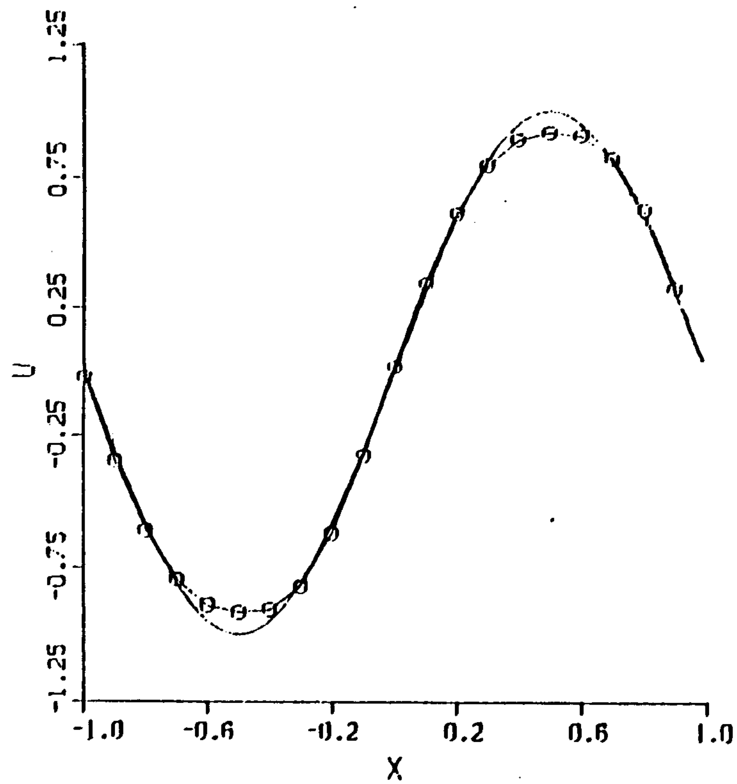

Figure 2b.

Figure 2. Numerical solutions of $u_t + u_x = 0$, $u(x,0) = \sin \pi x$ at $t = 2$, with $N = 20$ and $\tau/h = 0.8$. (a) UID2. (b) TID2.

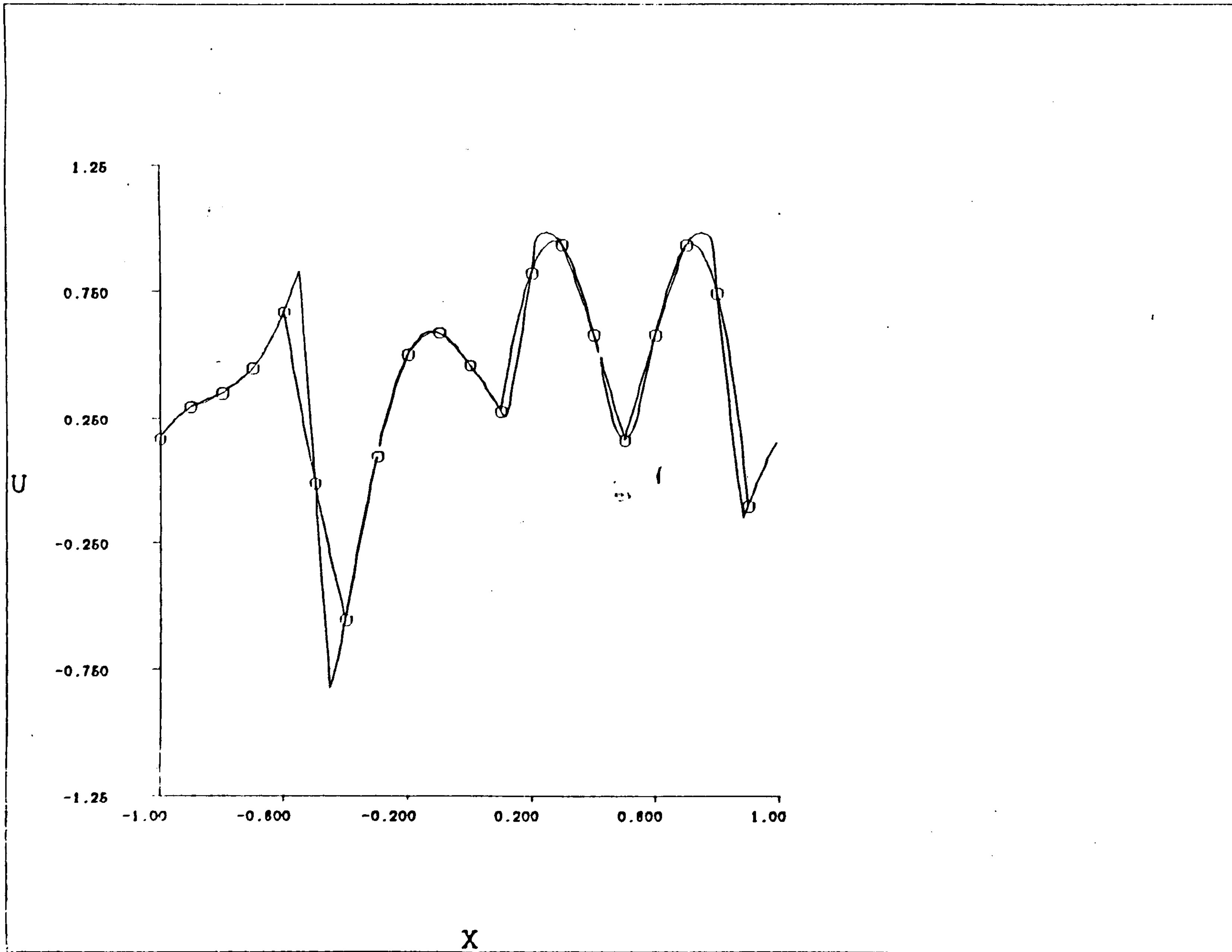

Figure 3a. $Q(x;\bar{u})$ for u given by (7.7) with $N = 20$

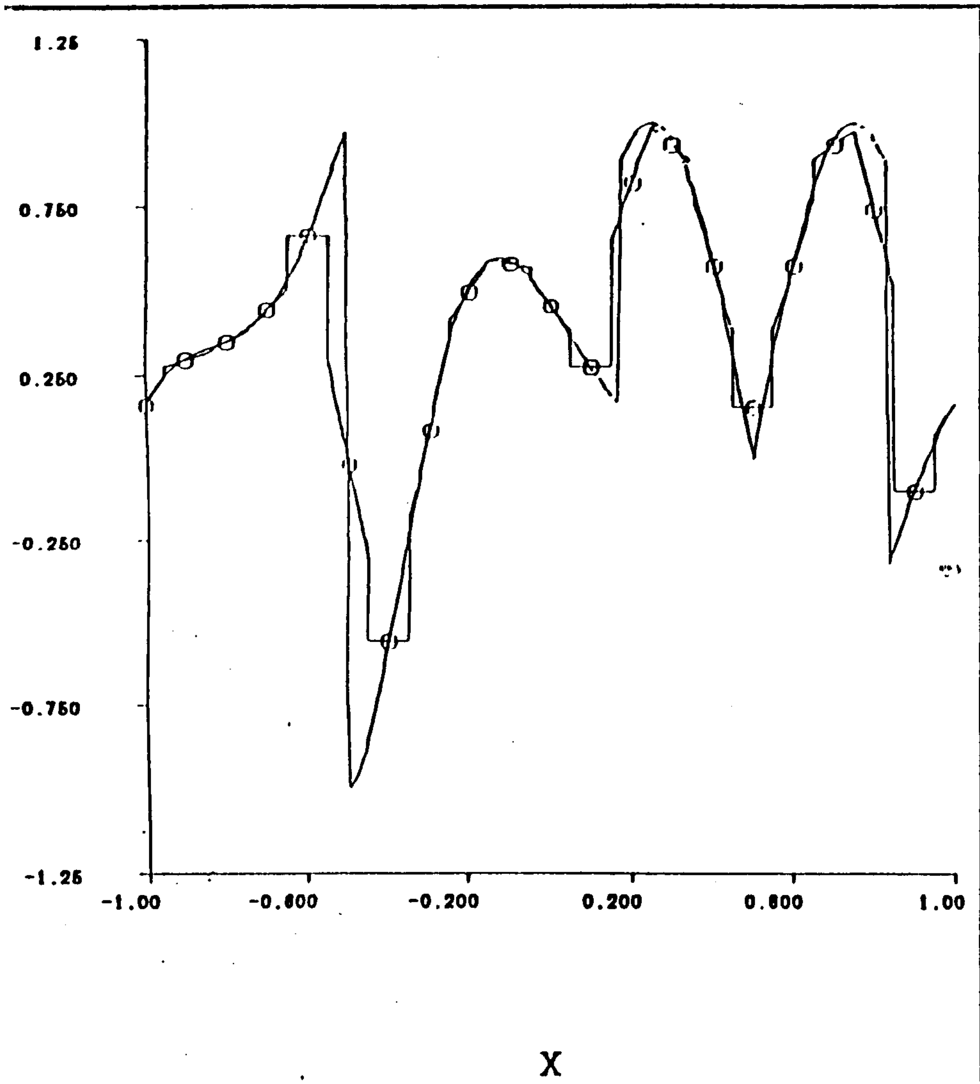

Figure 3b. $L^{UNO2}(x;\bar{u})$ for u given by (7.7) with N = 20.

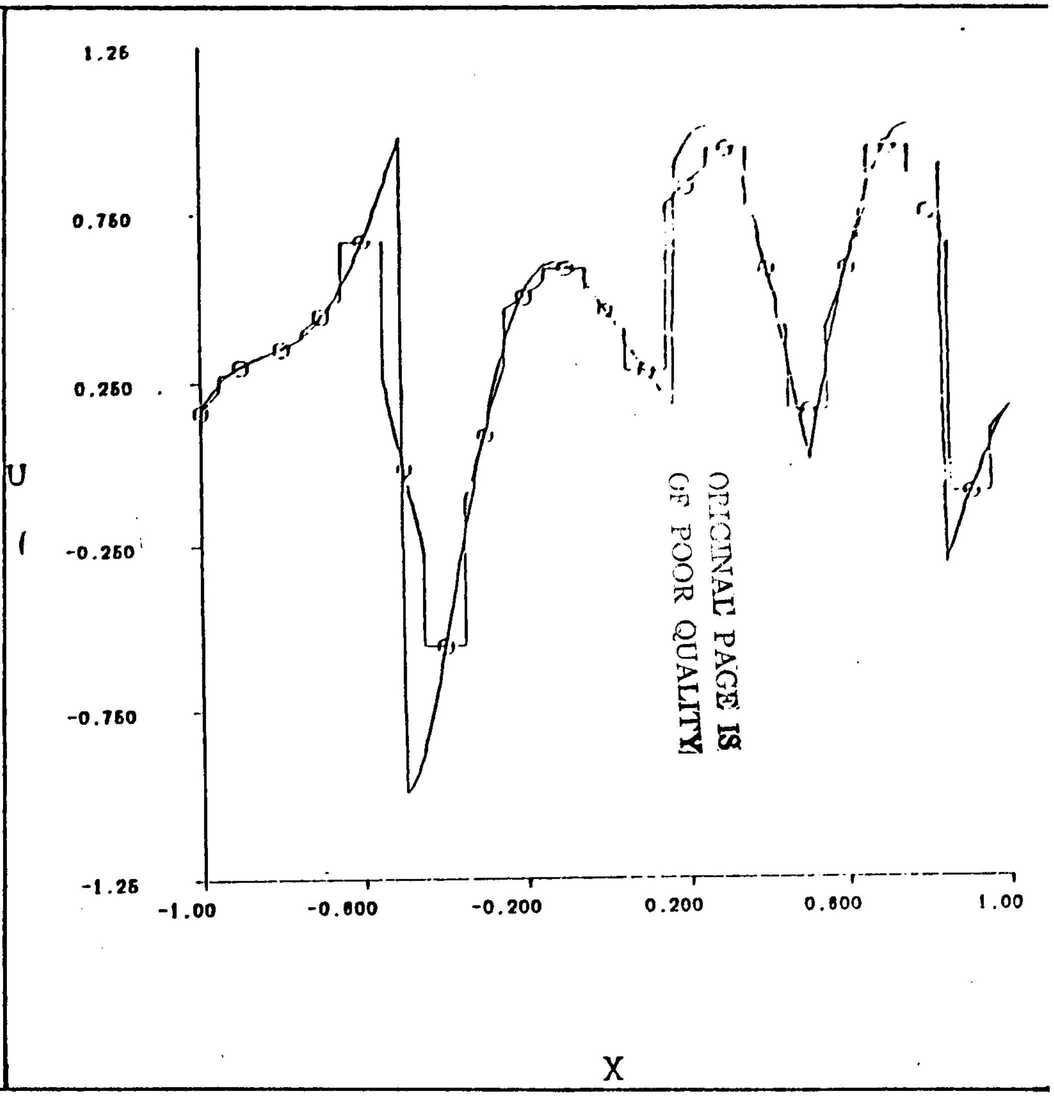

ORIGINAL PAGE IS OF POOR QUALITY

Figure 3c. $L^{TVD2}(x;\bar{u})$ for u given by (7.7) with N = 20.

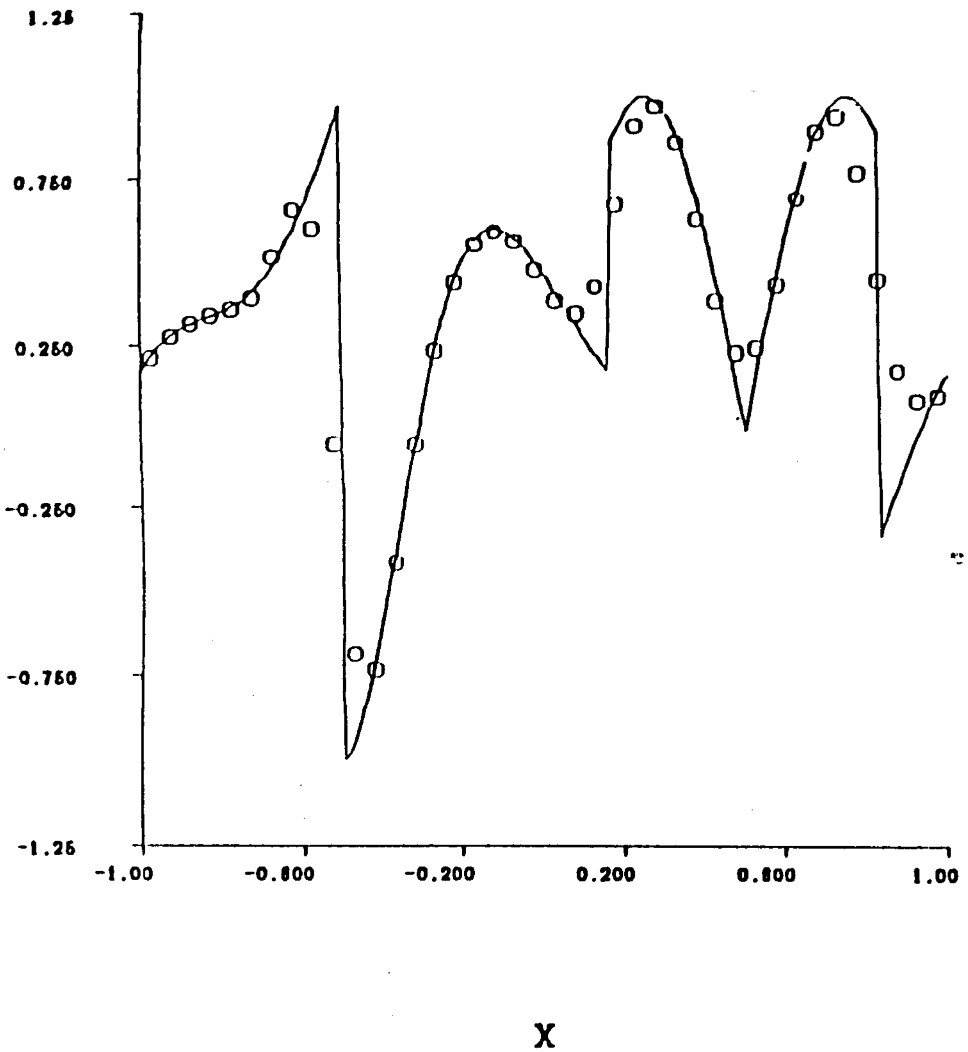

Figure 4a. Numerical solution of $u_t + u_x = 0$, $u(x,0)$ defined by (7.7) at $t = 2$ with periodic boundary conditions $N = 40$ $\tau/h = 0.8$, using UNO2.

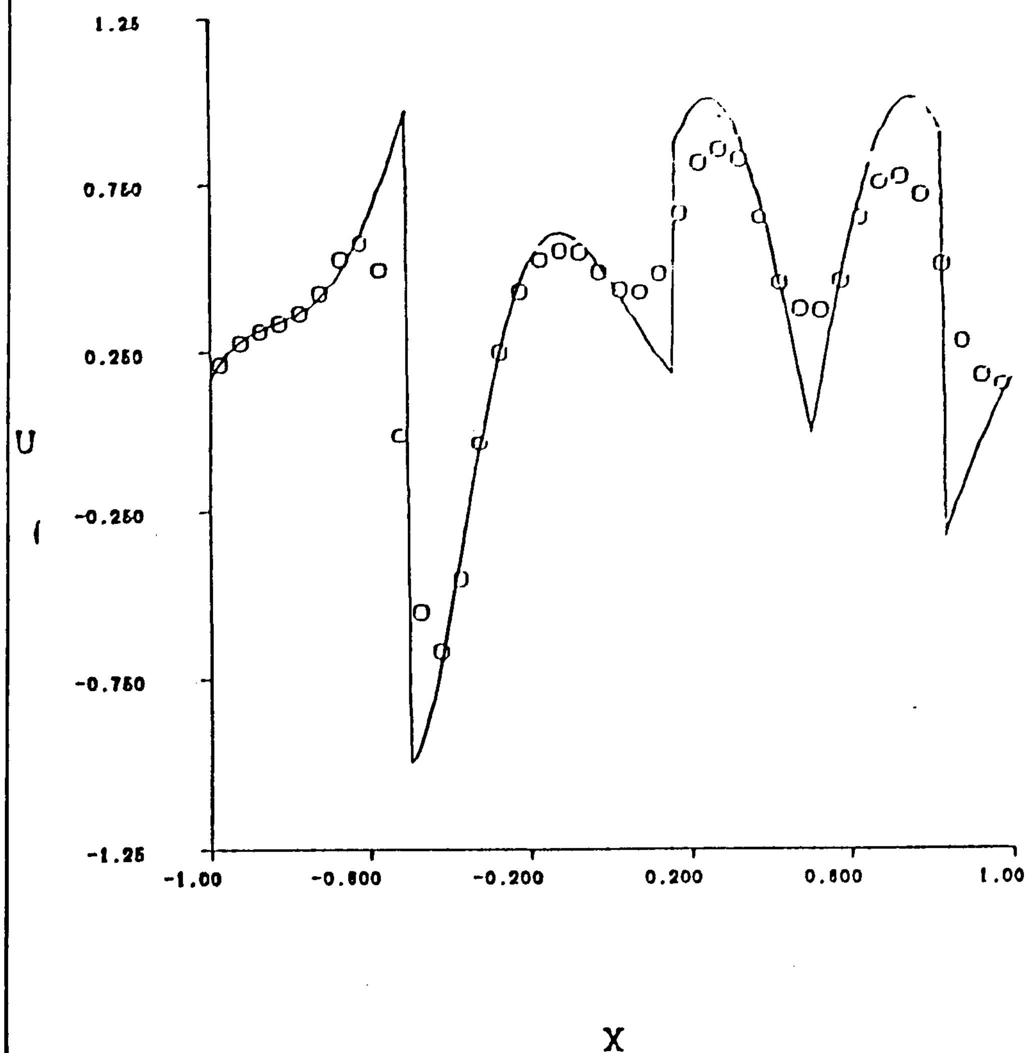

Figure 4b. Same as Figure 4a using TVD2.

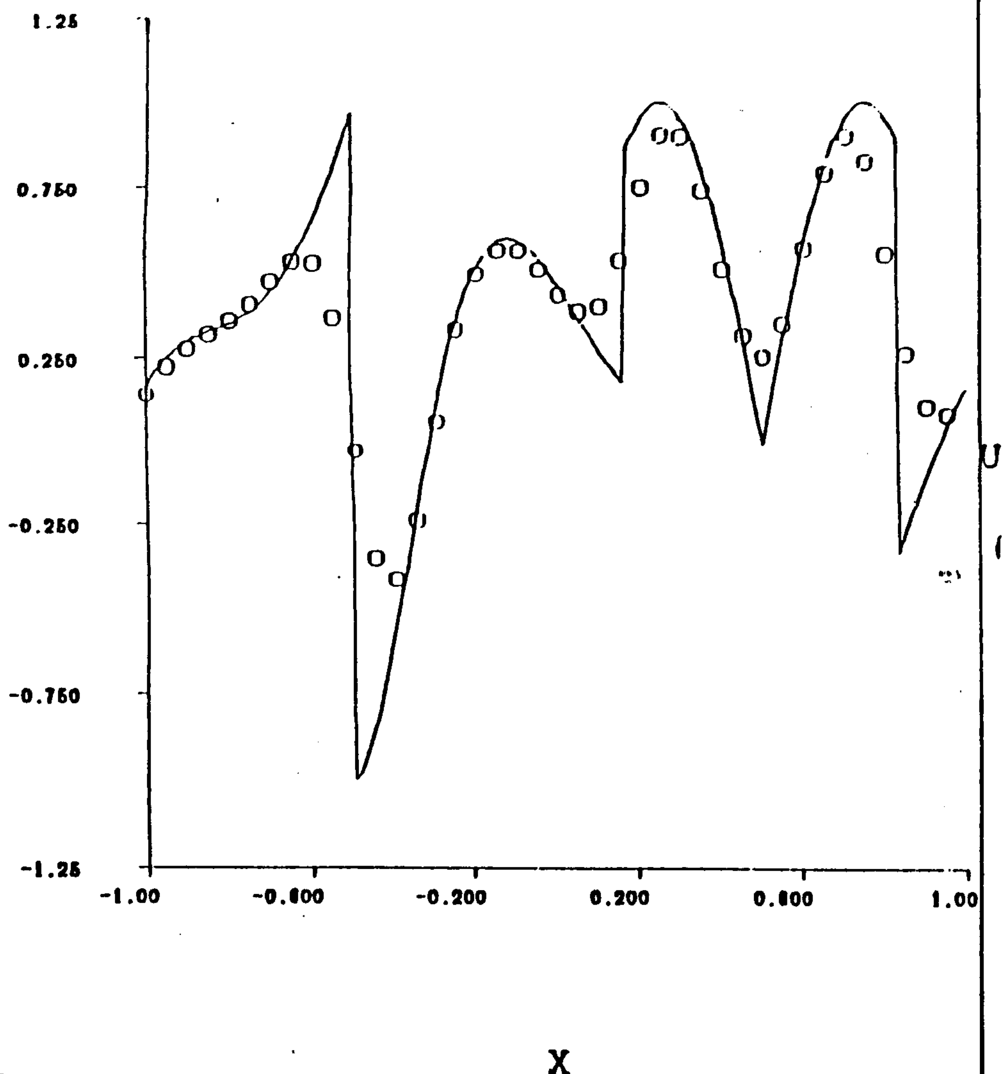

Figure 5a. Same as 4a except with given data at $x = -1$, and outflow at $x = 1$.

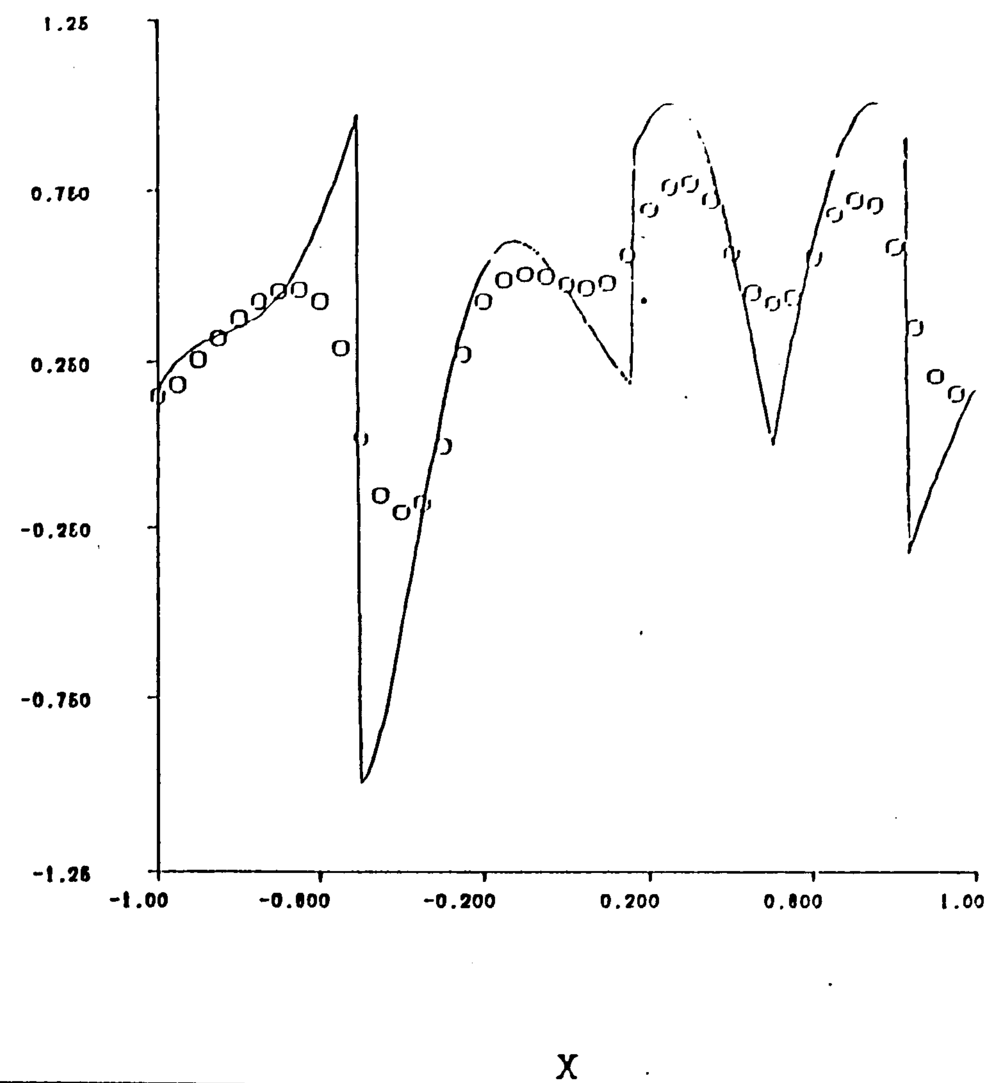

Figure 5b. Same as 4b except with given data at $x = -1$ and outflow at $x = 1$.

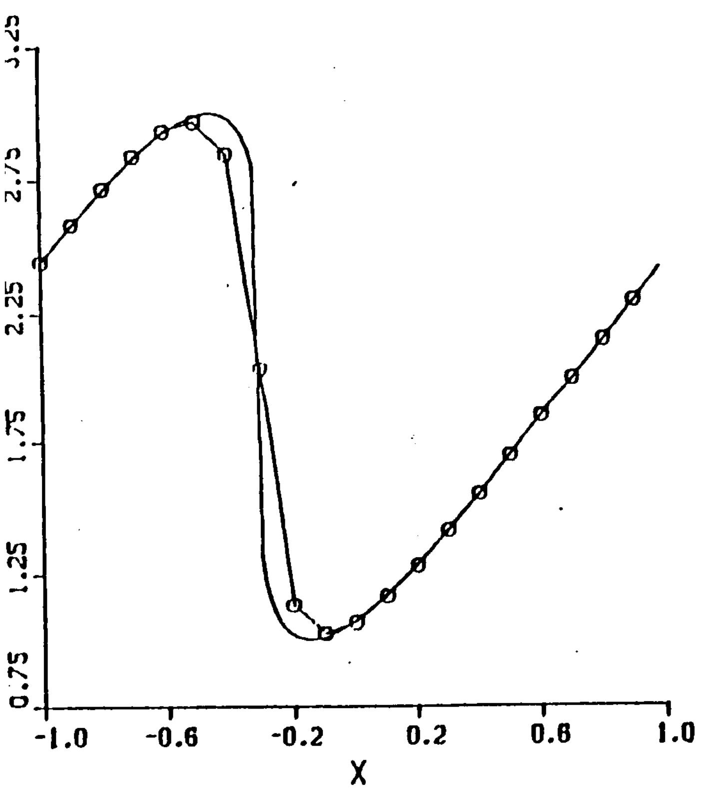

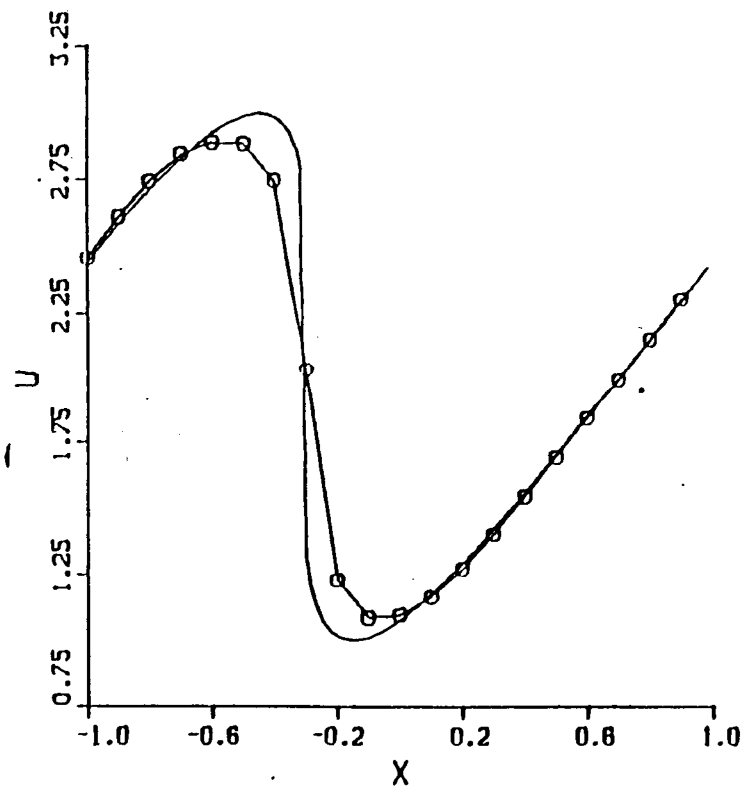

Figure 6a. Solution to (7.8) with $\alpha = 2$, $\beta = 1$, $N = 20$, CFL# = .5, at $t = 0.35$ using UNO2.

Figure 6b. Same as Fig 6a using TVD2.

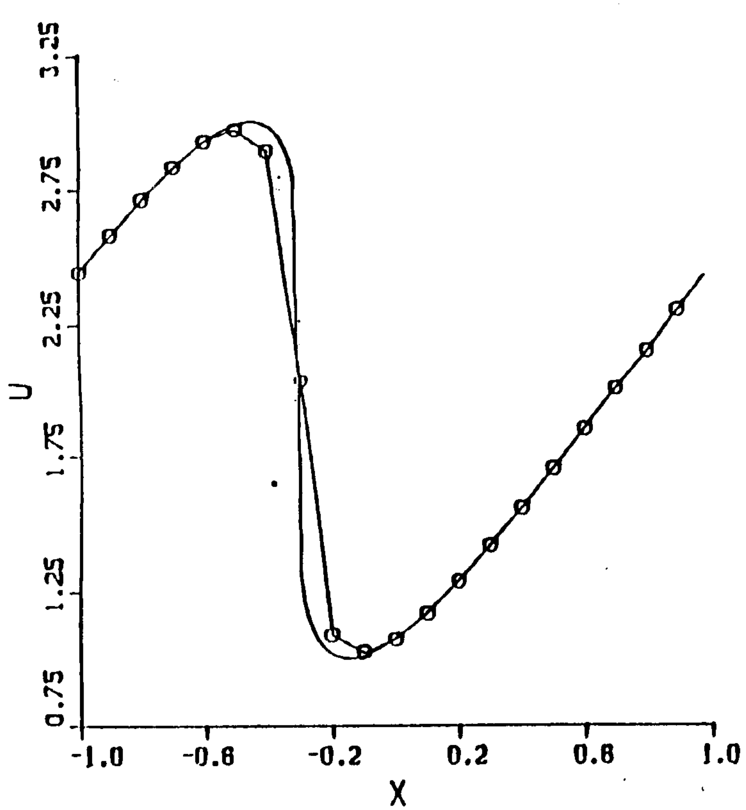

Figure 6C. Same as Fig. 6a using FNO2.

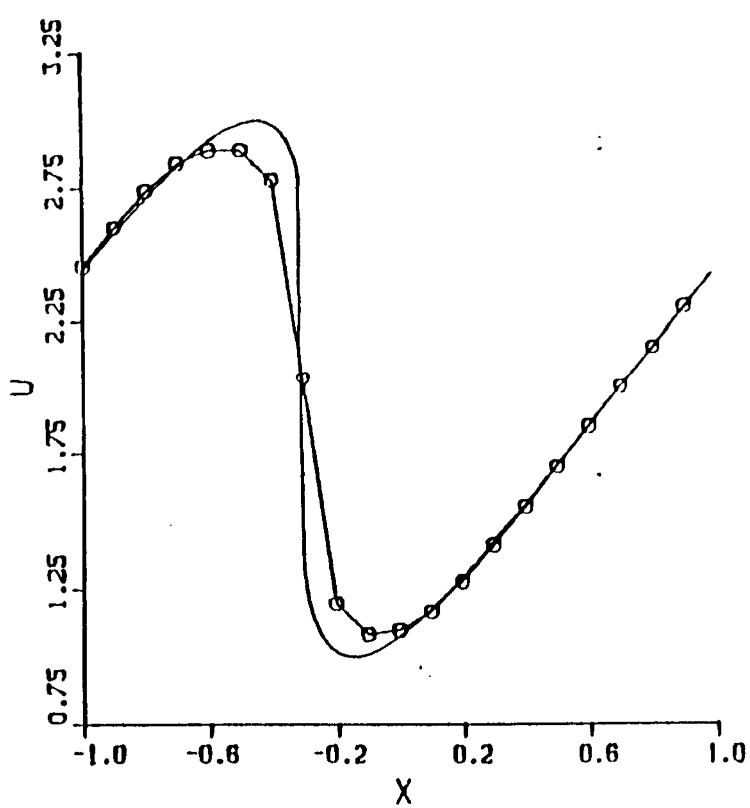

Figure 6D. Same as Fig. 6a using FVD2.

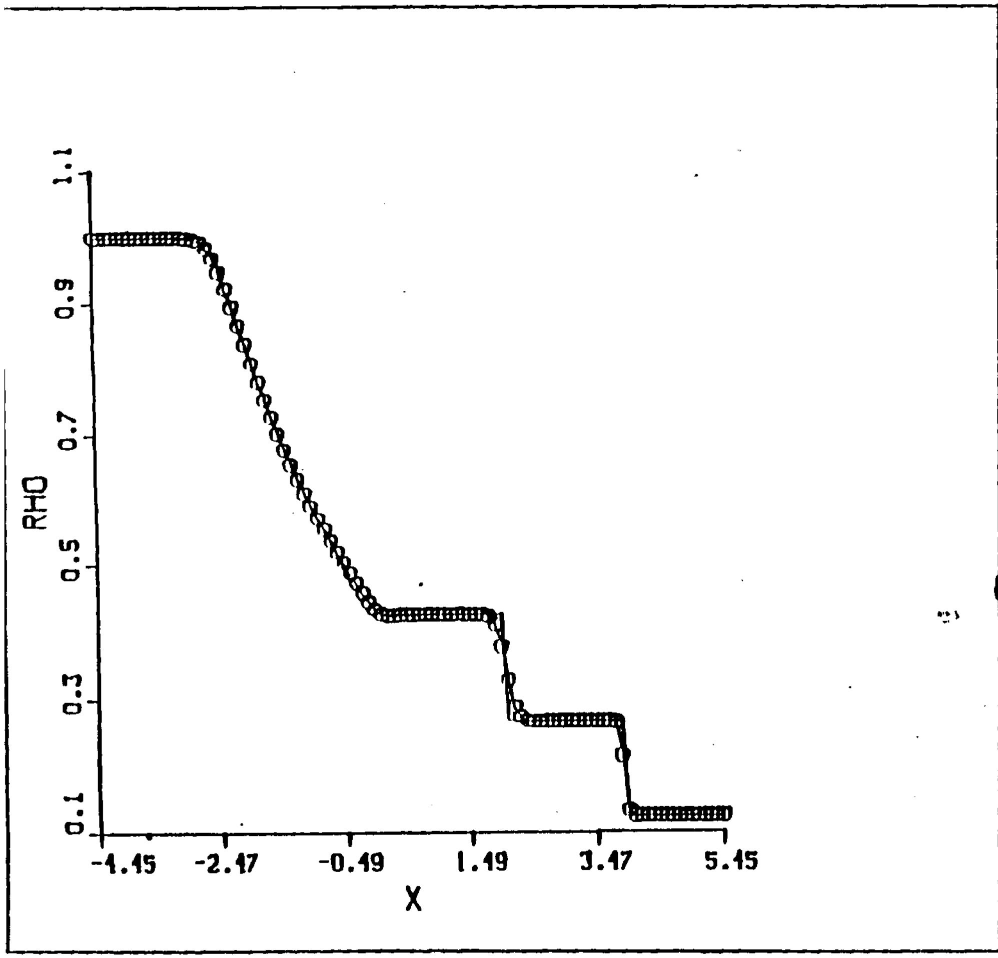

Figure 7a.

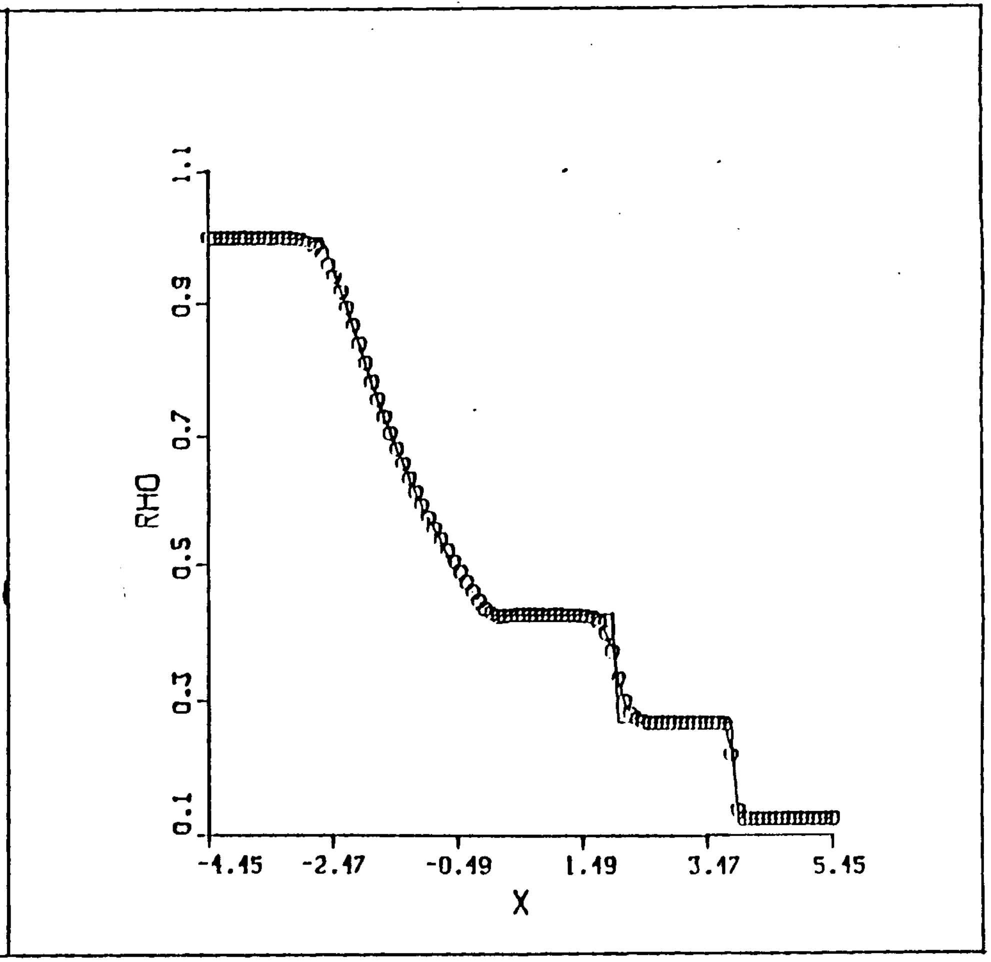

Figure 7b.

Figure 7. Numerical solution of density in a Riemann problem for Euler's equations.
(a) UN02 (b) TVD2

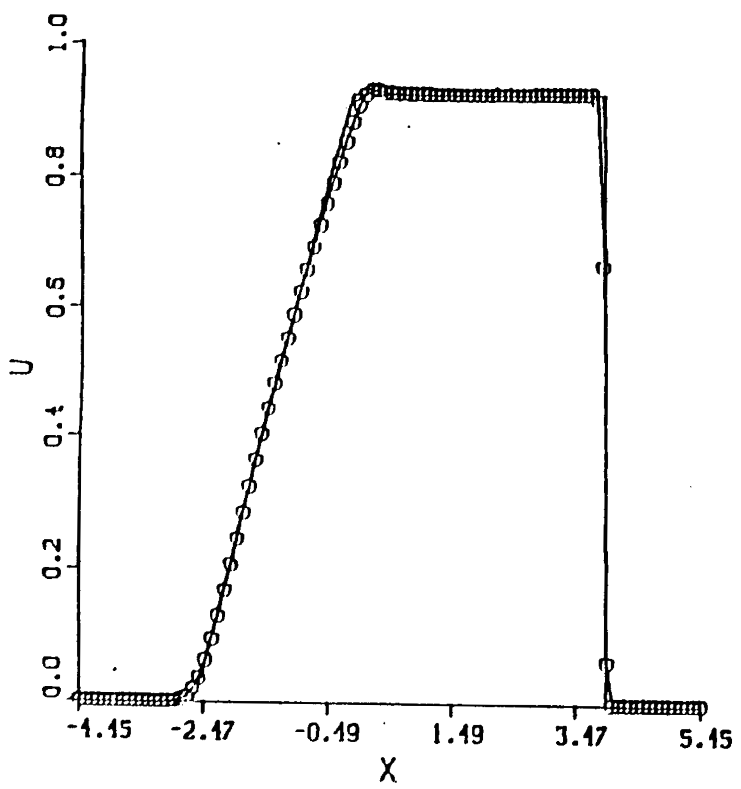

Figure 8a.

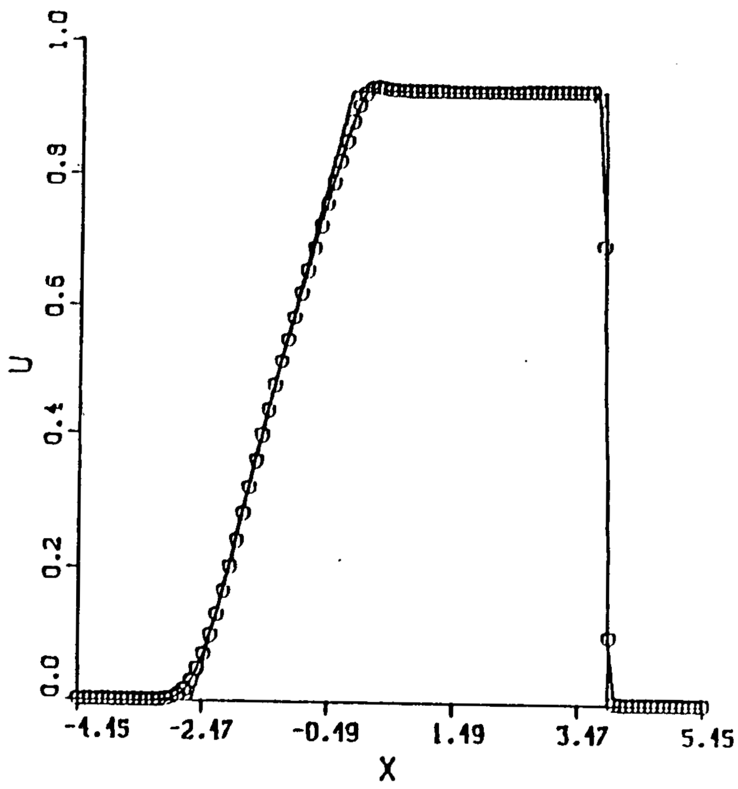

Figure 8b.

Figure 8. Numerical solution of velocity in a Riemann problem for Euler's equations. (a) UNO2. (b) T D2.

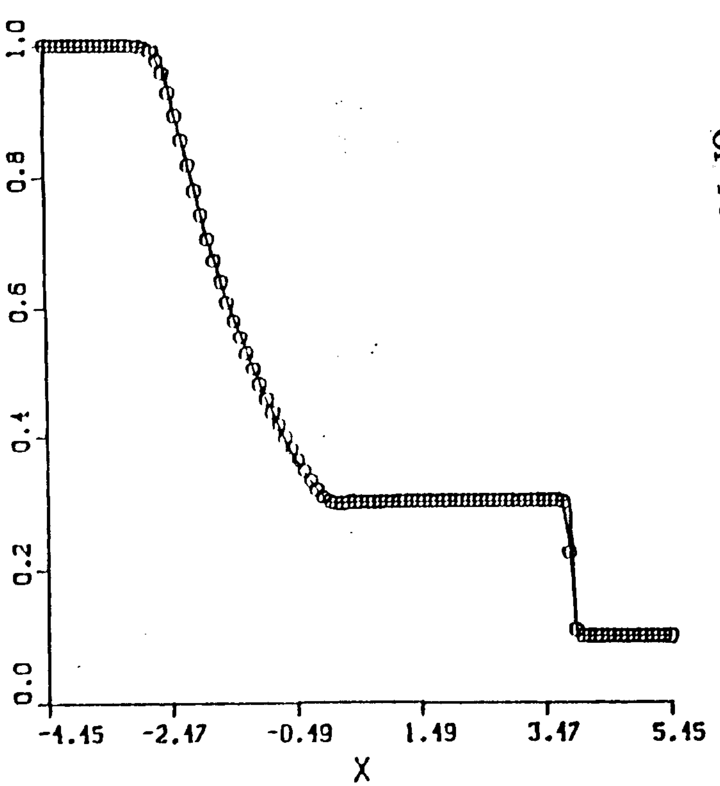

Figure 9a.

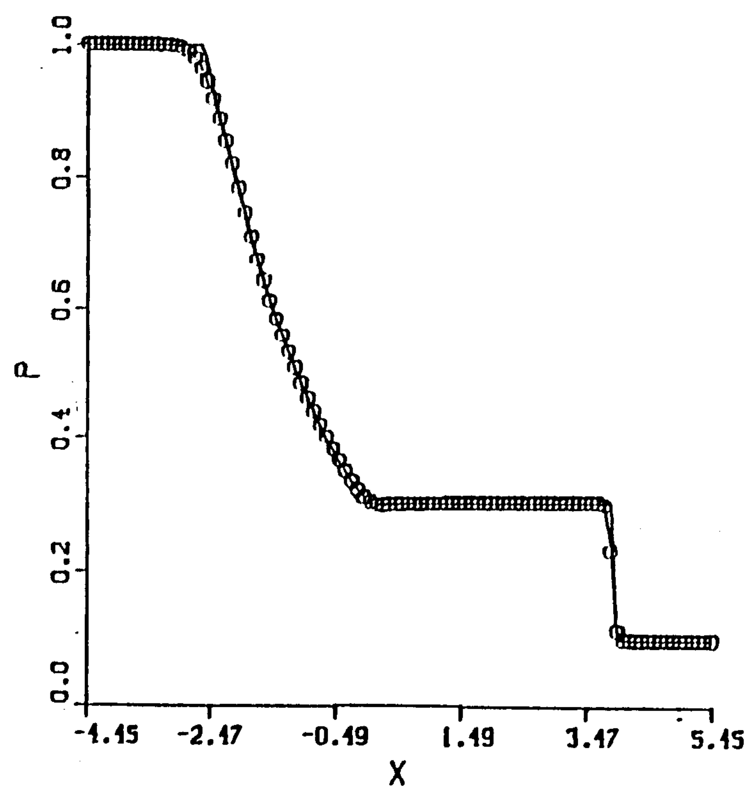

Figure 9b.

Figure 9. Numerical solution of pressure in a Riemann problem for Euler's equations. (a) UNO2. (b) TVD2.